

The Evolution of Hymenopteran  
Wings: The Importance of Size

by Bryan N. Danforth

1983

Submitted to the Department of Entomology  
and the Faculty of the Graduate School of the  
University of Kansas in partial fulfillment of the  
requirements for the degree of Master of Arts

THE EVOLUTION OF HYMENOPTERAN WINGS:  
THE IMPORTANCE OF SIZE

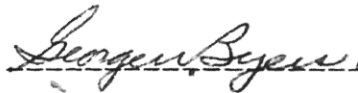
by

Bryan N. Danforth  
B.S., Duke University, 1983

Submitted to the Department of  
Entomology and the Faculty of the  
Graduate School of the University  
of Kansas in partial fulfillment  
of the requirements for the degree  
of Master of Arts.



-----  
Professor in Charge





-----  
Committee Members

-----  
Date thesis accepted

## Abstract

The allometric relationships between body size and several aspects of wing morphology in the insect order Hymenoptera were investigated using multivariate morphometric techniques. The study focused primarily on wing allometry in five monophyletic genera of bees (Perdita, Halictus, Ceratina, Trigona and Apis), but the patterns of size-related evolutionary change found within each of these genera are also found to exist in numerous other hymenopteran lineages. Aspects of wing morphology which scaled allometrically include (1) wing venation (relative stigma area and wing vein pattern) and (2) wing outline (aspect ratio and the location of the centroid of wing area). Both a strictly developmental and an adaptational explanation for these repeated patterns of size-related evolutionary change are considered. It is most likely that the repeated allometric trends result from adaptive change in wing morphology due to size-related changes in the physical properties impinging on the organism -- principally the quality and magnitude of drag. The fact that similar wing morphologies among distantly related species can result from similarity in body size has important implications for the study of

hymenopteran systematics, especially when numerous wing characters are employed and alternative phylogenetic hypotheses are evaluated on the basis of parsimony.

## Acknowledgments

I am very grateful to the people whose interest, support, encouragement and scepticism made this project possible. It was a pleasure to work in the lab of Dr. William Bell for much of this study. He and his students have provided invaluable facilities and advice for the past two years. Drs. Steven Vogel (Duke University), Richard Strauss (University of Michigan), and especially Richard Cloutier, Drs. Norman Slade, Jack Schlager and Chuan-Tau Lan contributed tremendously to my statistical and aerodynamic education during the course of my masters program. For the loan of specimens I thank Drs. Jerome Rozen (American Museum of Natural History) and Jack Liebherr (Cornell University Insect Collection). The graduate students in the Snow Entomological Museum, especially Jim Pakaluk, Bill Wcislo, John Wenzel and Doug Yanega, were extremely helpful in formulating the approach used in this work. Students in the Divisions of Herpetology and Ichthyology in the Dyche Museum of Natural History, especially Richard Cloutier, Linda Dryden, Linda Ford, Kate Shaw and Andrew Simons contributed essentially in scientific and personal ways. I am grateful to Andrew Simons for his help in clarifying parts of the discussion and for careful reading of the

final draft. Finally, the members of my committee. Drs. George Byers, Rudolf Jander, Charles Michener and Ed Wiley, as well as critically reading the text of my thesis, have made my graduate education at the University of Kansas challenging and rewarding. It is impossible to thank Dr. Charles Michener enough for his generosity and biological insight.

I thank my parents for their support and encouragement, and for the interest in nature which has brought me so much pleasure.

My dearest thanks go to Paula Mabee.

## Table of Contents

Introduction.....	8
Materials and Methods.....	11
Wing venation.....	11
Wing planform.....	14
Body weight and wing loading.....	16
Results.....	18
Wing venation.....	18
1. The stigma.....	18
2. Wing vein pattern.....	20
Wing planform.....	29
1. Aspect ratio.....	29
2. Position of centroid of wing area and aerodynamic center.....	30
Body weight and wing loading.....	32
Discussion.....	34
Wing venation.....	43
1. The stigma.....	43
2. Wing vein pattern.....	49
Wing planform.....	53
1. Aspect ratio.....	53
2. Position of centroid of wing area and aerodynamic center.....	55
Miscellaneous considerations.....	57

Systematic implications.....	65
Tables.....	67
Appendix.....	81
Figures.....	82
References.....	105



## Introduction

The scientific study of insect wings exhibits a strange dichotomy. On the one hand, a huge literature exists on comparative wing morphology, primarily due to taxonomic works. As observed by MacGillivray (1906), "the record [of insect evolution] is spread out [on the wings of insects] as on a printed page and only awaits the translator." Perusal of modern works on insect taxonomy and systematics will confirm that insect systematists continue to follow MacGillivray's advice. On the other hand, we have the literature on insect flight, an extensive body of knowledge on how a few species generate the forces necessary for flapping flight. Few studies have attempted to bridge the gap between these fields by investigating how wing structure relates to wing function. (Examples include Bartholemew and Casey, 1978; Casey and Joos, 1983; Casey and May, 1983; Casey, May and Morgan, 1985; Ellington, 1984a; Kingsolver and Koehl, 1985; Nachtigall, 1977, 1979; Norberg, 1972; Vogel, 1966, 1967a, 1967b; Weis-Fogh, 1973; and Wootton, 1979, 1981.) As a result, we know very little about what biological factors underlie the bewildering structural diversity shown by the wings of insects. The question "Why does this insect have this

wing morphology?" is rarely asked and more rarely answered. The research presented below was undertaken in order to determine the extent to which body size plays a role in the evolution of insect wings.

A change in body size, by profoundly altering the physical characteristics of an organism's environment, is known to be a major factor contributing to evolutionary change. (Calder, 1984; Peters, 1983; and Schmidt-Nielsen, 1981 provide reviews of the implications of body size.) The insect order Hymenoptera contains over 100,000 species of wasps, ants and bees which range in body length from 0.6mm (Mymaridae) to over 60mm (Megachilidae, Pompilidae), and is therefore an ideal group in which to study the evolutionary importance of body size. Indeed, the results presented below indicate that, to a large extent, the structural diversity in hymenopteran wing morphology, ranging from almost total veinlessness in the Platygasteridae, to elaborate vein complexity in the Symphyta, results from a number of specific size-related patterns of evolutionary change. By identifying convergent evolutionary trends in numerous independent lineages resulting from similarity in body size, this study illuminates, for the first time, the importance of body size to the evolution of wasp and bee wing morphology.

As a result of the universality of these size-related evolutionary changes, one can predict fairly accurately how the wings of large and small members of a given taxon will look. This does not mean that all Hymenoptera of a given size are identical; non-size-related, historical (phylogenetic) features are evident as well as those determined by size, at least at higher taxonomic levels.

## Materials and Methods

For morphometric analysis I selected monophyletic lineages containing relatively similar species while showing a wide range in body size (e.g. ten-fold or more range in body mass). These same criteria were applied by Kokshaysky (1974) in a study of the functional morphology of bird wings. The following bee genera were used: Perdita (Andrenidae), Halictus (Halictidae), Ceratina (Anthophoridae) and Trigona (Apidae). A sample of 41 specimens of Halictus ligatus from localities ranging from Panama to Michigan, USA was also analysed in order to compare intra- with interspecific wing allometry. The genus Apis (Apidae), although showing a small range in body mass (approx. seven-fold), was included because an extensive literature on Apis morphometrics already exists. Species investigated within each lineage, and the sample sizes are listed in table 1.

### Wing venation

Pinned specimens, primarily from the Snow Entomological Museum, were relaxed in humidity chambers and both wings from one side were removed. After cleaning by sonication in soapy water the wings were dry-

mounted on microscope slides. For weighing, specimens were removed from pins and oven dried as described below. Both specimens and slides were labelled for later reassociation. With a Leitz projecting microscope the wing outline, 20-30 points representing specific vein intersections and sclerites, a rough tracing of the vein pattern and a scale bar were drawn. The vein intersections and sclerites represented by these points were unambiguously homologous among all the species of a given lineage and are therefore homologous points (h-points) in the sense of Strauss and Bookstein (1982) and Bookstein et al. (1985). (For a recent critique of the concept of h-points see Read and Lestrel, 1986.) The projected images were checked with an ocular grid for optical distortion, which was not observed. The Cartesian coordinates of approximately 200 points describing the wing outline (digitizer in continuous input mode) and the 20-30 h-points were input to a Vector microcomputer using a digitizer pad. In coordinate files of this type fore and hind wings were treated separately. From these coordinate files the following variables were calculated: the distance between pairs of h-points (accurate to less than 4% of the value obtained using a binocular microscope with an ocular micrometer); forewing length (R), the distance from the center of the fused

radial and costal veins to the wing tip; the sum of forewing area and hindwing area on one side ( $S/2$ ); and the area of the stigma ( $S_s/2$ ). The algorithm for calculating the area delineated by a string of points is given by Jennrich and Turner (1969). Figure 1a illustrates a plot of the contents of a typical coordinate file of this type, and how forewing length ( $R$ ) is defined. The points along the wing margin distally represent the intersections of the weakly sclerotized last abscissae of the medial, cubital and vannal veins with the wing margin. The appendix lists abbreviations for certain variables and parameters used in this study.

For analysis of allometric change in wing venation, Jolicoeur's multivariate generalization of the bivariate allometric equation based on principal components (PC) analysis was used (Jolicoeur and Mosimann, 1960; Jolicoeur, 1963a, b; Shea, 1985). The elements of the first unit eigenvector of log-transformed variates (Jolicoeur's first vector of direction cosines), when the first PC axis corresponds to overall size, represent allometric coefficients analogous to the single allometric coefficient used in bivariate studies --  $x$  in the equation

$$Y = bX^x.$$

eqn. 1

A null hypothesis of multivariate isometry can be constructed ( $H_0: \mathbf{b}_1 = (1/\sqrt{p}, \dots)$  where  $p$  = number of variables used) and a  $\chi^2$  test of deviation from isometry can be applied (Anderson, 1963 -- in Jolicoeur, 1963a, p. 17). In addition, the specific variate set chosen to describe the wing venation corresponded to the truss network advocated by Strauss and Bookstein (1982) and Bookstein et al. (1985). The desirability of this approach as compared to the more traditional type of multivariate data set is discussed by Strauss and Bookstein (1982). Thus each wing cell (an area delineated by veins in insect wings) was treated as a polygon (or truss) with four or more sides and, in some cases, two diagonals (fig. 19 illustrates the specific variables chosen for a typical wing). This provided a fairly complete description of wing vein pattern. Principal components analysis was performed using Minitab and BMDP on the University of Kansas' Honeywell mainframe computer.

#### Wing planform

Analysis of wing planform (outline of the wing pair approximately as it appears in flight), in order to

contrast the aerodynamic properties of wings of different shapes, followed the approach of Ellington (1984a, paper II). Fore and hind wings were coupled together as in flight, dry-mounted on microscope slides and drawn as described above. A digitizer pad was used to input the Cartesian coordinates of 400-500 points along the wing outline from which fifty chords at intervals of  $0.02R'$  along the span of the wing could be calculated. Unlike the aforementioned coordinate files, in these files the wing base is taken to be the proximal end of the forewing radial sclerite and wing length,  $R'$ , is the distance from this point to the forewing tip. Figure 1b illustrates a plot of the contents of a typical coordinate file of this type and how wing length,  $R'$ , and wing chord,  $c$ , are defined. This definition of the wing base, and thus wing length, differs slightly from Ellington's (1984a) in order to eliminate the ambiguity associated with defining the basal hinge line; the values were none the less very similar to those of Ellington for Apis mellifera (see Table 5).

These data were used to calculate aspect ratio and the non-dimensional radii of the first, second and third moments of wing area for diverse groups of Hymenoptera using the algorithms given by Ellington (1984a). Aspect ratio,  $4R^2/S$ , is one measure of wing shape, describing



how elongate/narrow or short/broad the wing is. The radius of the first moment of wing area represents the spanwise position of the centroid of wing area -- how wing area is distributed along the long axis of the wing. The convention among aerodynamic engineers is to indicate a point at this spanwise position and one quarter chord from the leading edge of the wing. This point represents the aerodynamic center used in aeroplane design and is indicated on all accompanying wing illustrations. Because the wing base is defined slightly differently in the two types of coordinate files described, values of  $R$  and  $R'$  calculated from the two files are not identical for the same species (e.g.,  $R$  for Trigona amalthea is 10.38 [table 1] while  $R'$  for the same species is 10.98 [table 5] --  $R'$  approximately 5% higher than  $R$ ) and thus aspect ratio calculated from the two types of data file ( $AR$  and  $AR'$ ) are not identical for the same species. However, within a given data set values for different taxa are comparable, and conclusions drawn from the two data sets are in agreement.

#### Body weight and wing loading

To measure dry body weight, specimens were oven dried at 50°C until the largest specimens reached a constant

(minimum) weight over two consecutive weighings (3-4 days). Weights were measured to the nearest 0.1 mg. In order to estimate the actual live weights supported in flight from the dry weight data, the relationship between freshly killed weight and dry weight was determined for 277 bees and other Hymenoptera (covering a range of body weights from 2.0 mg to 600.0 mg). Insects were killed in a cyanide jar containing one or two fresh leaves (to keep the humidity close to 100%) and within thirty minutes transferred to air-tight containers also containing a leaf. The containers were kept in an ice-filled cooler until weighing, which occurred within two hours of capture. These specimens were then oven dried as described above and weighed for comparison with wet weights. All weights and weight-related values (e.g., wing loading) are estimated live weights based on the regression equation calculated from these data.

Wing loading,  $p_w$ , equals the estimated live body weight ( $m_{wet}$ ) divided by total wing area ( $S$ ) and reflects the weight supported by a unit of wing surface (in  $g/cm^2$ ).

## Results

This study indicates that at least four discrete aspects of wing morphology change in predictable ways with evolutionary change in body size: relative stigma size, wing vein pattern, aspect ratio and the spanwise location of the centroid of wing area. How each of these features relates to body size is explained below.

### Wing venation

#### (1) The stigma

The stigma is a heavily sclerotized spot on the leading edge of the forewing, bordered by wing veins. Stigma area scales negatively allometrically - small species within most lineages have disproportionately large stigmata. Figures 2a-f show the relationship between the log of stigma area ( $S_g/2$ ) and the log of total wing area on one side of the body ( $S/2$ ) for the five lineages and H. ligatus. Table 1 gives the means and standard errors for log wing area and log stigma area for each species and table 2 gives the equation for each group. An exponent of 1.0 would indicate isometry and values less than 1.0 indicate negative allometry. The departure from isometry is statistically significant in

all lineages except Perdita and Apis and is significant for H. ligatus. Qualitatively, the negative allometry in stigma area is quite clear in comparisons of large and small members of each of the five lineages (cf. Fig. 12a and b, 13, 14, 16, 17).

The ubiquity of negative allometry in stigma area among other hymenopteran groups which possess stigmata is demonstrated by comparisons of large and small members of these groups: Tenthredinidae (Ross, 1937), Ichneumonidae (Fig. 3), Braconidae (Fig. 4, Praon is a member of the subfamily containing the smallest braconids), Megaspilidae, Sphecidae (Fig. 8, Sphecius speciosus is one of the largest sphecids; Fig. 9, 10; also see Bohart and Menke, 1976, Fig. 41 and 47 for illustrations of minute sphecids), Pompilidae (Fig. 7, Pepsis is among the largest Hymenoptera), Colletidae (Fig. 11) and Anthophoridae (Fig. 15). In addition, there are no large Hymenoptera (greater than 2 cm wing length) known to the author with very large stigmata. Furthermore, in other insect groups, large stigmata appear to be associated with small body size: aphids (Aphidoidea: Homoptera) and psocids (Psocoptera).

The largest species of Perdita, P. bequaertiana (Fig. 12c), is very unusual in having a large stigma for its size. This species is unusual in a number of other

respects, to be discussed below.

## (2) Wing vein pattern

The multivariate analysis of wing vein pattern in the five bee lineages and qualitative investigation of other Hymenoptera indicate that the configuration of wing veins changes repeatedly in specific ways with evolutionary change in body size. In general, with increased body size the venation, especially the distal-most elements (cells SM2, SM3, M1 and M2, Fig. 18) become more elongate. Conversely, with evolutionary decrease in size the contrary holds -- the distal-most cells become reduced and withdrawn from the wing apex. This pattern is illustrated most strikingly in figures 3, 6-8, 11, 12a and b, 15, 16 and is summarized in fig. 20.

Tables 3 and 4 show the scaling (allometric) coefficients derived from the multivariate analysis. Each column represents the first unit eigenvector for a principal components (PC) analysis on the log-transformed measurements indicated in figure 19, and because these elements are of equal sign and similar magnitude, the first PC axis is interpreted as a size axis. Thus, by Jolicoeur's (1963b) method, each value represents an allometric coefficient analogous to  $\alpha$  in equation 1. Values greater than the null hypothesis (a unit

eigenvector with all elements equal to  $1/\sqrt{p}$ , where  $p$  equals the number of variables) indicate positive allometry, and values less than the null hypothesis indicate negative allometry. Although it is impossible to test for the significance of a specific value, each unit eigenvector was found to deviate highly significantly from the null hypothesis by the  $\chi^2$  test described in Materials and Methods.

In order to interpret these results it is necessary to break the wing venation down into its parts, the wing cells (see Figs. 18 and 19). The radial and first cubital cells together comprise the forewing base and are represented by variables R-1 to Cu1-2 in table 3. Measurements such as R-1, R-4 and Cu1-2, which lie parallel to the long axis of the wing, are referred to below as "longitudinal;" measurements such as R-2 and Cu1-1, which are more or less perpendicular to the long axis of the wing, are referred to below as "transverse." In general the basal portion of the forewing appears to scale roughly isometrically except for R-2 and Cu1-1, both transverse measurements, which show negative allometry. Halictus ligatus shows both of these trends intraspecifically as well. This results from a narrowing in these cells in larger species or individuals relative to smaller ones. Apis is exceptional in showing positive

allometry for R-2 (0.229).

The marginal cell becomes relatively elongate and narrow with increase in body size, as indicated by positive allometry in Marg-1 (Ceratina, Fig. 14), negative allometry in Marg-2 (Apis, Fig. 17, and Halictus, Fig. 13) or both (Trigona, Fig. 16, and Perdita, Figs. 12a and b). Analogous size-related changes in marginal cell shape have occurred in many other hymenopteran groups (cf. Figs. 3, 6, 9, 11, 15). This pattern, longitudinal measurements scaling positively allometrically and/or transverse measurements scaling negatively allometrically, is a trend seen in most wing cells.

The only general pattern of allometry seen in the first submarginal cell (R-2, SM1-1, SM1-2 and SM1-3) is the negative allometry of its proximal end (R-2), already mentioned in the description of the radial cell.

One of the most invariant and striking vein allometries is shown by the second submarginal cell (SM2-1, SM2-2, SM2-3 and SM1-2). Measurement SM2-1, representing the costal margin of the second submarginal, scales strongly positively allometrically within H. ligatus and in all lineages except Apis. This reflects distal movement of the attachment of the first r-m cross vein to the marginal cell with increased size. With

decreased size SM2-1 shortens markedly, which results in the second submarginal cell becoming triangular (e.g., Ceratina cockerelli, Fig. 14b; Perdita minima, Fig. 12b; and Neolarra californica, Fig. 15b). The fact that the second submarginal cell is often lacking in taxa with small body size may result from this allometric trend.

The third submarginal cell (SM3-1, SM3-2, SM3-3 and SM2-2), in those groups which possess it, in general becomes more elongate distally with increased body size. SM3-1 and SM3-3, both longitudinal measures, scale positively allometrically in general (H. ligatus differs slightly in showing negative allometry in SM3-1). Thus the second r-m cross vein, like the first, shifts distally on the marginal cell with increased size, and basally with decreased size (Figs 10, 12a and b, 14). The strong positive allometry in SM3-1 for Apis may have the same consequence for the position of the distal-most r-m cross vein on the marginal cell as the positive allometry in SM2-1 for the other lineages - to extend venation distally with increased size and to withdraw it proximally with decreased size.

As a result of the tendency for the submarginal cells to scale positively along the long axis of the wing, the venation extends closer to the wing apex in larger species. This is reflected in the allometry of



the region between the last submarginal cell (SM2 or SM3) and the wing margin (D-1, D-2, D-3 and SM3-2). In general, D-1, 2 and 3 scale negatively allometrically. Thus, even though the wing outline tends to become more elongate and narrow with increasing size (as will be shown below) the elongation and narrowing of the wing cells is more pronounced, resulting in the wing venation extending nearer to the wing apex with increasing size and withdrawing from the apex with decreasing size (both inter- and intraspecifically). See especially Figs. 3, 9, 10, 12a and b, and 15.

Both the first medial (R-3, M1-1, M1-2, M1-3, M1-4 and M1-5) and the second medial (M1-4, M2-1, M2-2, M2-3, M2-4, M2-5 and M2-6) cells show an elongation distally along their long axes with increased size in all lineages and H. ligatus (positive allometry in M1-1 and M2-1 and negative allometry in M1-2 and M2-2) -- a trend supported by many other lineages of Hymenoptera. The consequence of the positive allometry along the long axes of the cells is to extend the distal ends of the cells toward the wing apex, because basally (R-4) the wing veins scale roughly isometrically. That these four measurements (M1-1, M1-2, M2-1 and M2-2) are diagonals indicates that elongation and narrowing with increased size or foreshortening and broadening with decreased size result

from the transition between quadrate first and second medial cells, in small species, and narrow parallelogram-shaped first and second medial cells, in larger species (cf. Figs. 9-11, 14, 15). There is no marked allometry in the lengths of any of the veins comprising these cells (except perhaps M2-5), indicating that distal extension occurs primarily through a change in shape of the cells.

As in the wing region distal to the submarginal cells, the region distal to the medial cells (D-3 to 6) becomes foreshortened with increasing size due to the distal extension of the wing venation. This is indicated by the negative allometry of D-3 and D-5 in most lineages and H. ligatus. Apis and Trigona are exceptional in showing slight positive allometry in D-5. In Trigona, however, there is still a reduction in the venation distally with decreased size and an enhancement of venation distally with increased size through changes in the degree of sclerotization of veins rather than through changes in the position of veins. This is shown clearly in a comparison of Trigona amalthea, a very large species, and T. duckei, a very small species (Fig. 16).

Finally, the second cubital cell (Cu2-1, Cu2-2, Cu1-1 and M1-5) shows negative allometry in Cu1-1, mentioned in the description of the first cubital cell, and Cu2-1.

Table 4 shows the allometric coefficients, and

figure 19 the measurements to which they correspond, for the hind wing. In general, allometric trends analogous to those seen in the fore wing are also seen in the hind wing: elongation toward the wing apex and narrowing of cells with increased size, and contraction toward the wing base and broadening of the cells with decreased size.

For the groups investigated the hindwing includes at most two closed cells, the radial cell (R1-R7) and the cubital cell (R-6, Cu1-1 and Cu1-2). R-2 and R-4, both longitudinal vein measurements, tend to show positive allometry. R-3 and R-7, transverse measurements, scale negatively allometrically in H. ligatus and in most lineages (Ceratina being an exception in showing positive allometry in R-3). Figures 12a and b, 13, 14, 16 and 17 illustrate these trends for the bee genera studied and, as shown by figures 3, 9, 10 and 15, they occur commonly among other hymenopteran taxa.

The consequence of this elongation and narrowing with increased size is a decrease in the relative distance between the apex of the radial cell and the wing apex, which is reflected in the negative allometry of D-1 and D-2 for most lineages. Trigona is exceptional in showing positive allometry for D-1. However, the degree of sclerotization of the veins comprising the distal

portion of the radial cell in Trigona decreases with decreasing size, giving a result similar to that seen in the other lineages: a withdrawal of the distal-most venation from the wing apex with decreased size, and vice versa (Fig. 16). The negative allometry in D-4 (in all lineages except Trigona), D-6 and D-6+7 indicates narrowing of the wing with increasing size. D-5 of Trigona, however, corresponds more closely to D-4 of the other lineages than does D-4, because of Trigona's extremely small jugal lobe compared to the other groups, and it scales negatively allometrically. The negative allometry in R-7 and D-4 (D-5 for Trigona) together indicate negative allometry in wing width.

Although the congruence of intraspecific allometry in H. ligatus and interspecific allometry in the five lineages has been mentioned above, it is important to emphasize how closely allometry within H. ligatus agrees with interspecific allometry in Halictus. For the 53 total variables presented in tables 3 and 4, H. ligatus differs noticeably from the Halictus lineage in the direction of the allometry in only five (R-4, R-3, Marg-2, SM3-1 and R-3 in the forewing) and conforms closely in the most striking allometries (e.g., SM2-1: 0.239 in H. ligatus, 0.220 in Halictus). Thus, the allometric patterns observed interspecifically in the five lineages

and in other groups of Hymenoptera are also shown among the populations of a species ranging from Colombia to Canada (with body size increasing in a southerly direction).

In summary, the allometric trends in fore wing vein pattern which seem to hold generally for all or most lineages are the following: positive allometry in R-1, Marg-1, SM2-1, SM3-1, SM3-3, M1-1, M1-5, M2-1, M2-5; and negative allometry in R-2, Cu1-1, Cu2-1, Marg-2, D-1 to 3, M1-2, M2-2, and D-5. The following allometric trends hold for the hindwing: positive allometry in R-2 and R-4; and negative allometry in R-3, R-7, D-1, 2, 4, 6 and 6+7. These trends indicate that with increasing body size, for both fore and hind wings, the distal cells (marginal, second and third submarginal, first and second medial in the forewing, and the distal portion of the radial cell in the hindwing) become more elongate and narrow, resulting in a decrease in the distance between the distal-most wing veins and the wing tip. Fig. 20 summarizes these trends by indicating the predicted changes in vein conformation resulting from increased size. Reversal of arrows would indicate the shape changes accompanying decreased size. Large Hymenoptera which clearly illustrate these allometric trends are the Nyssoninae, especially Bembix and Sphecius (Fig. 9), the

Vespidae (often identified in keys by their elongate and narrow first medial cell, called the discoidal cell), Megarhyssa (Fig. 3) and other large Ichneumonidae, Bombus and other large bees (e.g., Figs. 11a, 15a, 17a) and the large pompilids such as Pepsis (Fig. 10). In Sphecius speciosus (Fig. 9) a unique extra r-m cross vein is found in the hindwing of the largest specimens, further supporting the existence of the trend toward enhanced distal wing venation with increased body size. Similarly, in many species of Perdita there is sexual dimorphism in body size and in wing venation: females are larger and have a fully developed last abscissa of Cu (M2-5) and second m-cu cross vein (M2-4) while males are smaller, with these two veins, comprising the distal extent of the second medial cell, weakly sclerotized (nebulous, to use the terminology of Mason, 1986). One would expect similar sexual dimorphism in wing venation in other hymenopteran groups in which body size is sexually dimorphic.

#### Wing planform

##### (1) Aspect ratio

Aspect ratio increases with increased body weight in

all lineages and within H. ligatus, as shown by figures 21a-f. Mean body weight and mean aspect ratio and the standard errors for all species are given in table 1. Because the relationship tended to be curvilinear in some cases (Trigona and Halictus) and because body weight was normally distributed in only three groups (Halictus, Apis and H. ligatus), non-parametric tests of association were used. The relationship was shown to be statistically significant, by Olmstead and Tukey's corner test or Kendall's coefficient of rank correlation, for all groups except Perdita ( $p < 0.10$ ) and Apis ( $p < 0.10$ ). Thus, large body size, in general, tends to result in more elongate and narrow wings, and small body size tends to result in broader wings. That this positive association is a general feature of hymenopteran evolution is illustrated in table 5. In all groups from parasitoids to Apidae, the smaller species have lower aspect ratios than their larger relatives (cf. Figs. 3-17).

(2) Position of centroid of wing area and aerodynamic center

The centroid of wing area tends to be located more proximally in large species and more distally in small species. The distance of the centroid from the wing base, as a fraction of total wing length, is given by  $r_1$ .

the non-dimensional radius of the centroid of wing area. Figure 22 shows the relationship between  $r_1$  and wing length,  $R'$ , for the 51 taxa listed in table 5 (statistically significant negative association between  $R'$  and  $r_1$  by Olmstead-Tukey's corner test:  $p < 0.002$ ). Negative association between  $r_1$  and wing length reflects the tendency for the wings of small Hymenoptera to be broad and bluntly spatulate (extreme examples of this trend are Mymarommatidae and Mymaridae, Chalcidoidea) while the wings of larger Hymenoptera tend to be more narrowly elongate and tapered apically (cf. Figs. 3-6, 9, 11, 12a and b, 15, 16). The use of  $r_1$  in the description of the wing shapes of flying animals was first suggested by Ellington (1984a). His data on 19 taxa of birds and insects (Table 1, paper II) show a similar negative association between wing length and  $r_1$ , although he did not mention this. The similarity of  $r_1$  values for Apis mellifera in the present study ( $0.485 \pm 0.002$ ,  $n=5$ ) and Ellington's study ( $0.480 \pm 0.002$ ,  $n=5$ ) suggests that the two data sets are comparable. The same close correlation between  $r_1$  and  $r_2$  (the non-dimensional radius of the second moment of wing area) and between  $r_1$  and  $r_3$  (the non-dimensional radius of the third moment of wing area), referred to as "laws of shape" by Ellington, were observed in the present study.



Considering the allometric changes in wing venation and wing outline together, one sees a remarkably non-intuitive result: while the distribution of wing area shifts in one spanwise direction with size change, the structural elements supporting the wing membrane, the veins, shift in the opposite spanwise direction. The consequence of this can be seen most clearly by comparing the positions of the aerodynamic center and the wing venation in large and small members of many groups of wasps and bees (Figs. 3, 6, 8-10, 12a and b). Although in general the aerodynamic center lies in the first medial cell, figure 15b (Neolarra, a minute nomadine bee) indicates that the aerodynamic center may even lie beyond the distal-most wing cells.

#### Body weight and wing loading

The relationship between dry body weight ( $m_{dry}$ ) and approximate live weight ( $m_{wet}$ ) calculated for the 277 bee and wasp specimens was

$$m_{wet} = 0.00034 + 2.79 m_{dry}. \quad \text{eqn. 2}$$

The correlation coefficient was 0.98. This equation was used to convert dry body weights of museum specimens to

approximate live body weight.

Wing loading tends to increase with increased body weight as shown by figures 23a-f. Means and standard errors for body weight and wing loading for all species included are shown in table 1. Like aspect ratio, the relationship between wing loading and body weight is curvilinear for some groups (Ceratina, Trigona and H. ligatus) so nonparametric tests of association were used. Only Perdita ( $p < 0.5$ ) and Apis ( $p < 0.1$ ) failed to show a statistically significant relationship between body size and wing loading.

## Discussion

In summary, based on the observed trends, one would expect decrease in body size within a clade or a species to result in the following changes in wing morphology: enlargement of the stigma, withdrawal of the venation from the wing apex, a decrease in aspect ratio and transition to a more spatulate planform. Likewise, with increased body size one would predict decrease in stigma area, extension of the wing venation toward the apex of the wing (primarily through elongation of the submarginal and medial cells), increased aspect ratio and a more acutely tapering wing tip.

How can the repeated allometric patterns in wing morphology be explained? Before considering answers to this question it is necessary to distinguish among several types of allometry. Gould (1966) recognized four: ontogenetic allometry, differential growth in individual ontogeny; evolutionary allometry, allometry among members of a single line of descent; intraspecific allometry, allometry among members of a single species (either within or between populations); and interspecific allometry, allometry among species of a single

monophyletic group at the same growth stage. It is important to realize that, although Gould uses "evolutionary allometry" to describe a type of allometry accessible only to paleontologists, and very rarely identified, "interspecific allometry" is an equally evolutionary phenomenon. The focus of the current study is interspecific allometry, allometry resulting from cladogenic evolution giving rise to descendants of varying size. What is the cause of the wing allometries described above? Two hypotheses seem plausible.

First, interspecific allometric patterns could arise simply through the extension of the ontogenetic or intraspecific allometry of an ancestral species over the range of body sizes assumed by its descendants. Thus the regression line for growth of variable  $y$  against body size in the ancestral ontogeny is simply extended at one or both ends as descendant species evolve different body sizes, with the slope of the line remaining roughly constant. Figure 24a illustrates this hypothesis using the terminology of Alberch, et al. (1979) and Kluge and Strauss (1985). Body size at onset of development of  $y$  ( $\alpha$ ) and at maturity ( $\beta$ ) and the slope of the allometric growth curve for variable  $y$  ( $k$ ) are shown for the ancestor (subscript 1) and three descendants (subscripts 2-4). The interspecific allometry of variable  $y$  in adult

individuals of the three descendants is shown by the dashed line and isometry is indicated by a line with  $k=1.0$ . The correspondence of ancestral ontogenetic allometry and interspecific allometry among the three descendants would be consistent with this hypothesis. In this example, attributing interspecific allometry to adaptation of the descendant species to the exigencies of their environments would not be the most parsimonious explanation. In the absence of further information (to be discussed below), a simpler explanation would be that the interspecific allometry arises because the ancestral ontogeny had a particular allometric trajectory, for whatever reason, and that the ancestral developmental program has been faithfully retained in the descendants. This concept has been reviewed by several authors (Cock, 1966; Gould, 1977; Huxley, 1932; and Simpson, 1953). Freedman (1962) found a correspondence between ontogenetic allometry and interspecific allometry in the primate genus Papio -- a result consistent with this hypothesis.

In quantitative genetic terms this hypothesis holds that genetic (including ontogenetic) correlations between morphological features and body size could result in interspecific allometry in those features solely due to a change in size. Lande (1979) reviews the theoretical and

empirical support for the idea that selection on body size alone can generate interspecific allometry in other features (brain weight in mammals). He concludes that within closely related forms (e.g., populations within a species or species within a genus) brain weight allometry arises solely from the genetic correlation of brain and body weight. However, interspecific allometry at a higher taxonomic level no longer agreed with the relationship predicted by the brain weight/body weight genetic correlation. This suggests that interspecific allometry at this level is due to selection directly on brain weight. Clearly this hypothesis should not be ruled out as an explanation of the interspecific allometries observed in the present study. Invariant interspecific wing shape allometries in distantly related lineages of Hymenoptera could be due to possession of similar wing shape/body size genetic correlations combined with evolutionary change in body size.

An alternative hypothesis holds that repeated interspecific allometric trends result from adaptation to the particular set of biological and physical forces resulting from each descendant's body size. Positive allometry in the cross-sectional area of tetrapod limb bones provides an allometric pattern consistent with this hypothesis. Under isometry, body weight increases as the

cube of length while cross sectional area of limb bones. and thus their strength, increases as the square of body length. If limb bones scaled isometrically large animals would have relatively weak skeletons compared to their smaller close relatives -- clearly undesirable to elephants. Thus, as Galileo (1637) recognized in the seventeenth century, the cross sectional area of limb bones scales positively allometrically such that larger tetrapods have relatively more robust leg bones. According to this hypothesis, the fact that an allometric pattern is repeated in numerous lineages, as are the wing allometries described here, indicates convergent evolution and suggests that adaptation to the physical environment imposed by body size is the cause.

Obviously, these two potential causes of interspecific allometry are not mutually exclusive; allometric trends in an ancestor's development could parallel those allometric relationships ultimately favored by natural selection acting on the body proportions of descendant species. But the fact that ontogenetic or intraspecific allometries may be adaptive over the size range of one species does not necessarily mean that the same allometric relationship would be acceptable as an interspecific allometry over the size range of a monophyletic group of its descendants. And, as Lande

(1979) pointed out, interspecific allometry at different taxonomic levels may have different causes.

How can these two hypotheses be distinguished? A first step would be to simply compare ontogenetic (or intraspecific, in the case of holometabolous insects) allometry to interspecific allometry. The genetic correlation hypothesis could be falsified if the ontogenetic allometry of one or more species (preferably basal members of a clade) is found to be different from the interspecific allometry observed in the same features among members of the clade. Figures 24b and c illustrate potential outcomes of this sort. Ontogenetic allometry of the ancestral species ( $k_1$ ) does not conform in either case to the interspecific allometry among its three descendants (shown by the dashed line). Offspring of the same parents would provide a series of individuals differing in body size but similar in genotype which would allow calculation of an intraspecific allometry comparable to the interspecific allometry. If possible, experimental manipulation (hormonally or nutritionally) of conspecific or confamilial larvae to produce dwarf or giant adults would give further insight into the ontogenetic correlations between body size and wing morphology.

Neither of these approaches was possible in the



present study. (Intraspecific allometry in Halictus ligatus reflects in part evolutionary allometry because the H. ligatus specimens come from populations ranging from the northern U.S. to Panama.) A final approach to the assessment of the influence of ontogenetic or intraspecific allometry on the interspecific allometric patterns described here is to identify the degree to which homologous elements of the wings of different groups scale similarly. For example, if extension of wing venation distally with increased size results from positive allometry in homologous veins in different groups, and positive allometry in other veins apparently could have achieved the same structural result, ontogeny is implicated as a source of that allometry. Alternatively, the ontogenetic hypothesis would be falsified if the overall pattern, extension of the wing venation distally with increased size, and vice versa, was achieved by non-homologous elements in different lineages. This seems to be the case in the present study. For example, although elongation and narrowing of both medial cells with increased size appears a common pattern in most hymenopteran groups, some large Hymenoptera show tremendous elongation only in the first medial cell (Vespidae, some Nyssoninae) while others show elongation primarily in the second medial cell (Pepsis,

Apis). As pointed out in the results, Trigona achieves results similar to the other lineages primarily through changes in the quality (degree of sclerotization) of the distal veins rather than through changes in their positions.

An adaptational hypothesis must ultimately be supported by functional information. This appears to be the case with size-related wing shape changes. The wing morphology characteristic of small wasps and bees seems to result from adaptation to the physical forces imposed by their size, and the reverse is true for the wings of large Hymenoptera. However, in order to understand the aerodynamic implications of a given wing morphology at a given body size one must understand how physical properties of the aerial environment change with body size.

For life in moving fluids, such as air and water, body size has profound implications -- most importantly on profile drag. (For an excellent presentation of fluid dynamics as it relates to biology, see Vogel, 1981.) Total drag on a flying animal is the sum of three forms of drag: (1) skin friction drag, resulting from shearing stresses in the boundary layer, (2) pressure drag, resulting from flow separation at the downstream surface of an object and subsequent net pressure opposing forward

movement and (3) induced drag, the drag resulting from lift production. Profile drag is the sum of skin friction and pressure drag. The coefficient of drag, a non-dimensional measure of drag, will be used in the following discussion because it allows easy comparisons between objects of different size. The profile drag forces experienced by an object moving through a fluid are determined both by the shape of the object and the flow properties of the surrounding fluid, which is expressed by Reynolds number ( $Re$ ). Reynolds number quantifies the relative contribution of inertial and viscous forces in a fluid medium. At high  $Re$  ( $Re > 10,000$ ) inertial forces predominate, flow is likely to be turbulent, boundary layers are thin and the coefficient of profile drag is low. With decreasing  $Re$  viscous forces become more important, flow is increasingly laminar, the boundary layer increases in thickness and the coefficient of profile drag increases, primarily due to increased skin friction drag (Vogel, 1981; Lissaman, 1983). Because the  $Re$  experienced by an organism is directly related to its body size (see equation 3;  $\rho$  = density,  $l$  = a linear dimension,  $V$  = velocity,  $\mu$  = viscosity), body size alone determines, in part, the magnitude of profile drag experienced by an organism.

$$Re = \rho lV/\mu \quad \text{eqn. 3}$$

In addition, because small objects present relatively more surface area to the fluid (due to the relationship of mass and surface area under isometry) the increase in drag coefficient resulting from decreased size is further enhanced. Thus, simply with change in body size the combined effects of change in Reynolds number and change in relative surface area cause significant changes in the nature and magnitude of drag experienced by flying animals. Reynolds number experienced by members of the Hymenoptera probably range from less than 100 for the smallest species, such as Mymaridae and Platygasteridae (Re = 200 for Drosophila: Vogel, 1967b) to over 5000 for the largest species, such as Pepsis and the largest Megachilidae (Re = 4000 for Schistocerca: Jenson, 1956).

#### Wing venation

##### (1) The stigma

The independent evolution of the stigma in a number of groups (Odonata, Psocoptera, Homoptera, Neuroptera and Hymenoptera) indicates that it is an important functional element of insect wings. The aerodynamic role of the stigma has been investigated in detail by Norberg (1972)

and his findings provide a possible explanation for the negative allometry observed in this study. Norberg found that, in dragonflies, the stigma has a mass greater than an adjacent region of wing membrane of equal area, and this is undoubtedly the case for the Hymenoptera. In addition, he found that the chordwise center of mass lies behind the torsional axis of the wing for all chordwise wing strips except at the position of the stigma where the center of mass lies in front of the torsional axis. Over-concentration of mass behind the torsional axis would lead to flutter at the top and the bottom of the stroke cycle and thus unfavorable (negative) angles of attack at the beginning of the following half-stroke. Norberg argues that the concentration of mass along the leading edge, the stigma, opposes flutter by balancing the mass on the opposite side of the torsional axis, thus passively maintaining a favorable angle of attack at pronation and supination. If Norberg's hypothesis holds for the hymenopteran stigma, the wings of small wasps and bees, with disproportionately large stigmata, would appear to enhance passive wing pitch regulation. This would be understandable if the wings of small Hymenoptera are subject to an unfavorable twisting moment. Such a twisting moment in small wasps and bees could arise in at least two ways.

First, if small hymenopteran wings have a center of mass further behind the torsional axis of the wing than larger Hymenoptera, a larger pterostigma would be required to offset the increased tendency to flutter. Although I have no data with which to test this hypothesis the decreased aspect ratio of small hymenopteran wings could have this effect if the relative broadening of the wing resulted primarily from an enlargement of the trailing portions of the wing.

Alternatively, an unfavorable pitching moment could arise if the relative positions of the torsional and mass axes are the same in small and large wasps but the wings of small wasps experience greater acceleration at pronation and supination, resulting in greater twisting forces on the wing. Increased acceleration of the wings at pronation and supination would arise simply through decreasing body size because of the relationship between body size and wing-beat frequency. Greenewalt (1960) accumulated data on wing-beat frequencies and wing lengths for a large number of flying animals and found an inverse relationship between wing length and wing-beat frequency. The same trend is shown if Greenewalt's (originally Sotavolta's, 1947 and 1952) data for the Hymenoptera alone are analysed. In that case, wing beat frequency is related to wing length as shown by

equation 4 ( $f$  = wing-beat frequency,  $R$  = wing length).

$$f = 3.03 R^{-0.808} \quad n=73 \quad \text{eqn. 4}$$

Thus wing-beat frequency increases with decreasing size, and vice versa. This indicates that the rate of pronation, vanned twisting at the top of the upstroke, and supination, costad twisting at the bottom of the downstroke, increases with decreasing body size. Extremely rapid twisting at the bottom and top of each stroke, given comparable mass and torsional axis positions, would impose greater unfavorable twisting forces on the wings. Increasingly unfavorable twisting forces, resulting from decreasing size, may require relatively large stigmata for the passive maintenance of favorable angles of attack. This seems the most likely explanation for the negative allometry observed in stigma area.

An additional hypothesis for this trend, which does not rely on the view that the stigma functions in wing pitch regulation, considers the role of overall wing inertia in flapping flight. With decreasing size, and thus increasing coefficient of drag, wing motions are increasingly opposed and a proportionally greater amount of energy would be needed to keep the wings of small

Hymenoptera moving. However, any mass added to the wing, especially distally, would increase the overall moment of inertia of the wing and given an initial acceleration the wing would move further. Because Hymenoptera have asynchronous muscles and an elastic thorax that stores kinetic energy in the form of stretched resilin fibers (Chapman, 1969), an increase of inertia in a wing experiencing high drag forces would be an effective way to enhance the recovery of energy initially invested to move the wing. The large stigmata of small Hymenoptera thus may increase the energy recoverable from the flapping wing at low Reynolds numbers.

Although Norberg's (1972) study fairly conclusively supports his hypothesis about stigma function in the Odonata, the wing morphology of the Hymenoptera suggests an alternative role for the stigma -- enhancing wing shape changes in flight. In all Hymenoptera with relatively complete wing venation and stigmata, a line of wing membrane flexibility, called the median flexion line, extends from the costal margin of the wing immediately proximal of the pterostigma (between the prestigma and pterostigma) into the first submarginal cell, and then runs parallel to the medial vein through the remaining submarginals. Where this line passes through veins ( $R_s$ , 1st r-m and 2nd r-m), regions of vein



weakening, alar fenestrae, are generally apparent. Such lines of weakening have been termed wing flexion lines by Wooton (1979, 1981) and are considered responsible for localized wing shape changes in flight, although this has only been demonstrated photographically for the claval flexion line in Wooton's papers (see Dalton, 1975, 1977). The location of the pterostigma, immediately distal of the medial flexion line, could enhance flexion at this point at the bottom and top of the stroke cycle, when the wing changes direction; the more massive the pterostigma, the greater this effect. Flexion of the leading edge of the wing would tend to generate leading edge vortices which could be important sources of unsteady-state lift. (For a clear review of the evidence in favor of unsteady state mechanisms of lift production in animal flight see Ellington, 1984b.)

Given that the relative size of the pterostigma increases with decreased body size in many groups, why do some of the smallest wasps, the majority of the Chalcidoidea, Proctotrupoidea (except Roproniidae, Proctotrupidae and Heloridae) and Cynipoidea (except Austrocynipinae), lack pterostigmata? At least one chalcidoid wasp, Encarsia formosa, has been shown to fly by a novel mechanism -- the 'clap-and-fling' mechanism of Weis-Fogh (1973; see also Ellington, 1975; Lighthill,

1973; Maxworthy, 1979). This mechanism involves wing movements quite different from those which take place in the forward flapping flight of larger animals, and generates lift by unsteady-state aerodynamic principles. Perhaps as a result of such wing motion, the structure associated with determining wing pitch in the standard model of wing motion, the pterostigma, has been lost. The flight of the Megaspilidae and the Austrocynipinae would be especially interesting in this regard because, although both are in superfamilies characterized by small size and no stigmata (Proctotrupoidea and Cynipoidea, respectively), both groups have tremendous stigmata. (The 'stigma' of Austrocynipinae is homologous to the marginal cell of other Hymenoptera but has been heavily sclerotized and thus resembles a true stigma.)

## (2) Wing vein pattern

Insect wing venation provides the structural support for the wing membrane. Wing veins, robust cuticular tubes which project above or below the surrounding wing membrane, carry circulating haemolymph and sensory nerves associated with wing sensillae. The observed changes in vein pattern associated with change in body size -- extension distally of distal wing cells with increasing size, and vice versa -- indicates a rearrangement of the

wing's structural elements as a result of changes in the aerodynamic forces impinging on the wing in flight.

The size-related changes in wing venation are in part due to the size related changes in wing outline. Increased aspect ratio would necessarily result in longer narrower cells, and vice versa. However, the changes in wing venation are more marked than would be predicted by change in wing outline alone, as shown by the relationship of the distal-most veins to the wing margin (negative allometry) and by qualitative comparisons of many groups (e.g., Neolarra and Thalestria, Fig. 15). The positive relationship between wing loading and body size (Fig. 23) could be one cause of this marked change in wing venation. With decreasing size wing loading, the force exerted per unit of wing area, decreases. Because the venation provides the support for this force, veins may be reduced as force per unit area decreases. If this were the case, one would expect the wing venation to become progressively fainter with decreased size and relatively more robust with increased size. However, this does not seem to occur. As figures 3, 9, 12a and b, 15 and 16 indicate, in most cases smaller members of groups have relatively more robust wing veins than their larger relatives. In addition, this hypothesis would not necessarily predict a change in vein configuration and

position.

A hypothesis which is consistent with the observed changes in the spanwise location of wing venation is related to changes in the bending moment of the wing with size. With increasing size, and thus increasing wing length, the bending moment of the wing increases. Prevention of potentially unfavorable bending of the wing, especially apically, may be the best explanation for the distal extension of wing venation in larger Hymenoptera.

Why then is the wing venation of small wasps and bees withdrawn from the distal portion of the wing? As indicated above, wing-beat frequency increases with decreasing wing length for most insects. Greenewalt (1960) attributed this relationship to the change in moment of inertia of the wing, which is related to wing length. Withdrawal of the relatively massive veins (as compared to wing membrane) most likely results in a decrease in moment of inertia below that predicted by decreasing wing length alone, especially at the smallest body sizes. In other words, because of allometric changes in wing vein pattern small Hymenoptera are likely to have higher wing-beat frequencies than would be predicted if large and small wings were simply scale models. (Equation 4 does not really allow testing of

this hypothesis because most of the species used in calculating it are quite large compared to the size range considered here.) Assuming the wing membrane is sufficiently rigid to resist unfavorable bending, increasing wing-beat frequency through decreased moment of inertia would result in an increase in the amount of thrust available. Because the movements of small wasps and bees are likely constrained by high coefficients of skin friction drag (see discussion of centroid of wing area below) maximizing thrust is of great importance.

Increased wing loading with increased body size has been found in most flying animals (birds: Fullerton, 1911; Greenewalt, 1962, 1975; Warham, 1977 -- bats: Greenewalt, 1975; Vaughan, 1970 -- insects: Greenewalt, 1975) and results from maintenance of approximate isometry between wing area and body mass. It is noteworthy that in studies of bird wing morphology results comparable to those found here for allometry of structural elements has been found. Warham (1977), measured the lengths of the humerus, ulna, manus and primaries for puffins of varying size. Analyzing his data by principal components analysis indicates positive allometry for humerus and ulna and negative allometry for manus and primaries ( $b_1 = (0.572, 0.596, 0.448, 0.342)$ ,  $n=21$ ;  $H_0 = (0.5, \dots)$ , 99.2% variance explained by the

first axis). Thus, as in Hymenoptera, the region of the wing distal to the structural elements (primaries) scales negatively allometrically while the structural elements themselves scale positively allometrically. Hertel (1966, p. 64) shows a comparison of a hummingbird and buzzard wing which indicates the same trend. Greenewalt (1975) similarly observed that wing weight scaled positively allometrically with respect to body weight for ducks and shorebirds, but not for passerines. He concluded that this reflects "substantial structural reinforcement as the size increases." Passerines were thought to differ in this respect because of their relatively low flight speeds.

#### Wing planform

##### (1) Aspect ratio

Aerodynamically, aspect ratio is an extremely important descriptor of wing shape, primarily in its relationship to the coefficient of induced drag, drag resulting from lift production. Because aspect ratio is in the denominator of the expression for the coefficient of induced drag (e.g. Clancy, 1975), high aspect ratio wings experience a smaller induced drag coefficient than low aspect ratio wings. High aspect ratio wings have

evolved repeatedly in large members of numerous lineages (see Table 5) which suggests that induced drag may become an increasingly important source of drag with increased body size. That this is indeed the case is suggested by at least two factors. First, wing loading, the mass supported per unit area of wing, increases with body size (Fig. 23). Therefore, in order to maintain a larger-bodied animal aloft, more lift is required per unit of wing area which results in a higher coefficient of induced drag. Second, the relative contribution of induced drag to total drag (induced plus profile drag) most likely increases with increasing size; primarily due to decrease in skin friction drag. Therefore, with increased body size and associated increase in Reynolds number, induced drag becomes a larger fraction of total drag. Minimizing the induced drag component of total drag, through high aspect ratio wings, is an apparently effective way for large Hymenoptera to reduce a major component of total drag. On the other hand, for small Hymenoptera total drag results primarily from skin friction, and the reduction in induced drag potentially brought about by high aspect ratio wings may have an insignificant effect on total drag. The repeated evolution of high aspect ratio wings in large Hymenoptera thus seems to be an adaptive change in wing morphology

resulting from a change in the drag properties of their environment.

Positive correlation between aspect ratio and body size is not unique to the Hymenoptera. Numerous studies in other animal groups have indicated a similar trend (Fullerton, 1911; Greenewalt, 1975; Warham, 1979). In addition to its effect on drag, aspect ratio has a relationship to flight performance. For birds and bats with low aspect ratio wings, flight is characterized by low speed and high maneuverability, while high aspect ratio wings are associated with higher flight speeds and gliding flight (Vaughan, 1970).

(2) Position of centroid of wing area and aerodynamic center

The fact that the centroid of wing area shifts proximally with increasing size and distally with decreasing size indicates that small wasps are devoting a larger portion of their wing area distally than larger wasps, and vice versa. Because wing area is proportional to the magnitude of the aerodynamic forces generated, the spanwise distribution of area, all else being equal, is related to the spanwise distribution of aerodynamic forces. According to Walker's (1925, 1927; also see Pringle, 1957) model of flight the majority of lift



arises from the proximal one-third of the wing and the majority of thrust from the distal two-thirds of the wing. This model fits the empirical results for the rook (Corvus frugilegus) reasonably well and also for data on locust and horsefly flight. The model gave less satisfactory results for mosquito flight, most likely due to the theory's neglect of induced wind, the airflow resulting from wing movement relative to the body, which would increase with increased wing-beat frequency (Pringle, 1957). To the extent that Walker's model holds for the Hymenoptera, the more paddle-shaped wings of small Hymenoptera would tend to enhance thrust production. Conversely, the more apically tapering wings of large wasps and bees would enhance lift production. One would expect that the wings of small Hymenoptera, living at low  $Re$  and thus exposed to strong profile drag forces, to emphasize thrust production. Because of their low wing loading and highly viscous environment, staying aloft presents no problem but getting anywhere -- from flower to flower or host to host -- presents a major constraint (Vogel, 1981). On the other hand, large Hymenoptera have high wing loading but are not as constrained by profile drag and thus the generation of lifting forces may be more important.

### Miscellaneous considerations

An additional aspect of wing morphology, wing surface sculpturing, bears some relationship to body size. For all airfoils the lift generated by translation through the air increases with increasing angle of attack (the angle formed between the wing chord and the oncoming wind). However, above a critical angle of attack, stall (a sudden drop in lift) occurs, due to separation of flow from the upper surface of the wing. Delay of flow separation, allowing higher angles of attack and greater lift is clearly desirable. Flow separation can be prevented or delayed through the generation of a turbulent boundary layer, and both large and small Hymenoptera have surface irregularities which probably accomplish this. Small Hymenoptera often have more elongate leading edge setae than their larger relatives, presumably due to the problems of generating turbulence in a thick boundary layer. That these setae indeed function in disturbance of the boundary layer is supported by the fact that surface roughness of a given size is most likely to disturb the boundary layer when located along the leading edge, as are these setae, where the

boundary layer is thinnest (Vogel, 1981). Conversely, large Hymenoptera, especially large bees, have wing papillae on the membrane beyond the distal-most cells which are lacking in smaller relatives (C.D. Michener, pers. comm.). In addition, the relative length of trailing edge setae increases with decreasing size. As shown by Figures 4-6 and 9, small wasps often have more elongate setae than their larger close relatives and the longest setae are localized along the trailing edge of the wing pair. This is carried to an extreme in the Mymaridae and Mymarommatidae (Chalcidoidea), the smallest Hymenoptera. Vogel (1967b) observed that length of wing fringe is associated with low aspect ratio in the Diptera and suggested that wing fringe resists the reversal of flow on the upper surface of the wing, which gives rise to stall. Wing fringe in small Hymenoptera may play a similar role -- allowing higher maximum angles of attack by resisting flow separation.

Much of the above discussion of the aerodynamic consequences of wing shape changes is based on the assumption that the mechanism of lift production for large and small wasps is the same, namely, that it is based on steady-state aerodynamics. This, however, may not be the case. An alternative hypothesis, explaining the observed patterns of wing morphology, is that

allometric changes in wing shape result from a transition between wings designed for the production of lift through steady-state mechanisms (in large species) and wings designed for the generation of lift through unsteady-state mechanisms (in small species). (For a review of the distinction between these two models of lift production see Ellington, 1984b.) Unsteady-state mechanisms which have been proposed include the delayed stall (Bennet, 1966, 1970), the 'clap-and-pling' (Weis-Fogh, 1973), and the 'flip' mechanism (Ellington, 1984a, b). Although our understanding of unsteady-state mechanisms of lift production is limited at this point, there is strong evidence that unsteady-state mechanisms are involved in several cases: the blowfly, Calliphora (Buckholz, 1978, 1980); the migratory locust, Schistocerca (Cloupeau, et al., 1979); and Odonata (Soms and Luttges, 1985). These and other studies indicate that unsteady-state mechanisms are capable of generating very large lift forces (far greater than those possible by steady-state mechanisms). Because the maximum lift to drag ratio obtainable by steady-state mechanisms decreases with decreasing  $Re$  (Clancy, 1975; Lissaman, 1983; Vogel, 1981), one might expect small Hymenoptera, living at low  $Re$ , to make use of unsteady-state mechanisms. One parameter used to estimate the

contribution of unsteady-state forces to flight is the reduced frequency,  $k$  (Maxworthy, 1981; Walker, 1925, 1927).

$$k = \omega(c/2)/V_{\max} \quad \text{eqn. 5}$$

Given that  $\omega$ , the angular velocity, increases with decreasing size (due to increased wingbeat frequency associated with small size, see above), and that  $V_{\max}$ , the maximum flight speed, decreases with decreasing size, equation 5 suggests that the reduced frequency is inversely related to body size. Smaller species may rely more heavily on unsteady-state mechanisms of lift production than larger species. If this is so, the morphological features associated with small size may reflect this. Norberg (pers. comm.) considers this a likely explanation for the changes in wing outline. He believes the features of small wasp wings (low aspect ratio, distal centroid) are associated with generating lift by the 'clap-and-fling' mechanism.

These patterns of wing allometry have not gone unnoticed by earlier workers. Rasnitsyn (1969; translation 1979) observed for the Symphyta that with decreasing size there is a strengthening of the costal margin of the wing and reduction in venation at the wing

apex and in the trailing portions of the wing (termed costalization by Rodendorf, 1949). In addition, he pointed out the enlargement of the stigma in small species. MacGillivray (1906) suggested that aspect ratio increases with increasing flight speed but does not comment on the role of body size. However, it is likely that forward flight speed increases with body size, which is the case in birds (Greenewalt, 1975). Interestingly, MacGillivray's presumed 'specialized' (i.e. derived) wing vein characters are almost all associated with large body size: elongate, narrow cells and small stigmata.

In spite of the apparent universality of the wing-scaling rules described above a number of exceptions exist. For example, the wings of nocturnal Hymenoptera show many features associated with small size in spite of the fact that nocturnal species are, in general, far larger than their diurnal close relatives. Perdita bequaertiana, noted earlier as anomalous in a number of ways, illustrates this phenomenon. Although P. bequaertiana is among the largest species of Perdita, it has a large stigma (Fig. 2a and 12c), a relatively low aspect ratio (Fig. 21a and 12c) and very low wing loading (Fig. 23a) -- all characteristics of small Hymenoptera. Unlike all other known species of Perdita the members of the subgenus Xerophasma (to which P. bequaertiana

belongs) are nocturnal. A number of other nocturnal Hymenoptera show similar wing features in comparison to their nearest diurnal relatives: Ophion (Ichneumonidae), moderately large body size and large stigmata compared to diurnal Ichneumonidae; Macrocentrus (Braconidae), large size, large stigmata, low aspect ratio and distal centroid (Table 5) compared with diurnal Braconidae; Megalopta (Halictidae), large size and large stigmata compared to Pseudaugochloropsis and other diurnal Augochlorini; and Sphecodogastra texana and S. noctivaga (Halictidae), large size and large stigmata compared to diurnal Evylaeus. In each case large nocturnal members of a lineage have wings with relatively large stigmata, low aspect ratios or distal centroids -- all characteristic of small size in diurnal species. Why would these exceptions be correlated with nocturnality? One possible explanation is that flying at night imposes different aerodynamic forces on insect wings and the wing morphologies of nocturnal species reflect adaptations to these physical properties. Alternatively, large nocturnal species may simply retain features of their smaller diurnal relatives. For thermoregulatory reasons the evolution of night-time activity may require the rapid evolution of large body size. If large body size is a recently acquired trait in these groups their wing

proportions may simply result from the retention of the wing features of their smaller, diurnal ancestors (as explained at the beginning of the discussion). Further investigation of this problem requires that we know more about the aerodynamics of night flight and the phylogenetic positions of these nocturnal groups.

It is clear from the discussion that wing allometry in Apis is unusual, differing from the other four genera in the allometry of several vein measures (e.g. R-2, SM2-1 and D-5 in the forewing) and in the size-related trend in the location of the centroid (A. laboriosa, the largest species, has a more distal centroid than A. florea, the smallest, Table 5). Why Apis is unusual is not clear, but it could be because the range of body sizes covered by this genus is fairly small compared to the other genera (resulting in the large and small members having nearly identical wing venation, Fig. 17). Probably more importantly, there are no species with very small body size (e.g. wing length of 5 mm or less), which is the range over which the allometric trends are most pronounced.

Throughout the Results and Discussion no suggestion has been made as to the direction of evolutionary change in body size in any of the five lineages studied. The history of evolutionary change in body size within a



lineage can only be understood in light of a phylogeny, which in most cases is lacking. However, for some groups it is possible to identify members for which large or small size is undoubtedly derived. The anthophorid tribe Xylocopini, large (20-30mm wing length), robust bees, is one of four tribes in the monophyletic subfamily Xylocopinae (Sakagami and Michener, in press). The other three tribes, Allodapini, Manuelini and Ceratinini, are all smaller in body size and, because the Xylocopini is not the basal group, its large size is most likely derived. The Xylocopini exhibits many of the features associated with large size in the morphometric analyses of other bees: minute stigma, elongate marginal, third submarginal and first and second medial cells, high aspect ratio and apically tapering wing. Contrarily, the genus Neolarra (Fig. 15b) in the anthophorid subfamily Nomadinae is extremely small. The majority of nomadines are larger and because Neolarra is most likely not a basal group (R.W. Brooks and C.D. Michener, pers. com.) its small size is presumed to be derived for the Nomadinae. It also conforms to the wing morphology predicted by the multivariate analysis. These and other examples in which the evolution of body size can be traced support the view that the observed patterns of wing allometry hold irrespective of the direction of

evolutionary change in body size.

#### Systematic implications

These results have important implications for the study of hymenopteran, and possibly pterygote, systematics because of the emphasis insect systematists generally place on wing vein pattern. For example, characters commonly used by bee systematists are relative length and width of the marginal cell (Marg-1 vs. Marg-2), length of the last free abscissa of the radius in the forewing (D-1), relative length and width of the medial cells and stigma size and shape. All these features of wing morphology are related to body size and thus do not necessarily represent independent evidence of common ancestry. The result of using characters closely related to body size is to artificially, and inadvertently, give weight to a single character: body size.

Phylogeneticists would be advised not to bias their results by including redundant characters in their data matrices when some single measure of body size might be more appropriate. Finally, it is common for hymenopterists in general to consider a large stigma the primitive state (e.g. MacGillivray, 1906). Because an enlarged stigma can clearly result from decreased body

size this hypothesis of polarity should be tested (e.g., by the outgroup criterion) in each case. Similarly, reduced wing venation, lack of certain veins or reduced sclerotization, is often considered a derived state. However, enhancement of wing venation could presumably arise as a result of increased body size and the structural requirements that it entails. Two groups in which this may have occurred are the Leucospidae (Fig. 5a) and large species of Trigona (e.g. Trigona amalthea, Fig. 16a).

Table 1. Means and standard errors aspect ratio (AR), wing loading ( $p_w$ ), area and log of stigma area.

Genus		
Species(n)	m $\pm$ SEM (g)	
<u>Perdita</u>		
<u>acapulcona</u>	(1)	
<u>albovittata</u>	(3)	0.0040 0.0003
<u>arcuata</u>	(3)	0.0048 0.0005
<u>beameri</u>	(3)	0.0052 0.0004
<u>bequaertiana</u>	(1)	0.0199
<u>bicolor</u>	(1)	
<u>bishoppi</u>	(4)	0.0033 0.0002
<u>californica</u>	(2)	
<u>chihuahua</u>	(1)	
<u>coreopsidis</u>	(3)	0.0074 0.0004
<u>cowaniae</u>	(3)	0.0082 0.0002
<u>interrupta</u>	(3)	0.0053 0.0004
<u>lateralis</u>	(3)	0.0054 0.0006
<u>laticauda</u>	(3)	0.0039 0.0002
<u>lingualis</u>	(3)	0.0122 0.0023
<u>maculigera</u>	(1)	
<u>maritima</u>	(3)	0.0185 0.0010
<u>mellea</u>	(1)	0.0026
<u>minima</u>	(4)	0.0021 0.0005
<u>obscuripennis</u>	(3)	
<u>octomaculata</u>	(5)	0.0091 0.0012
<u>portalis</u>	(3)	
<u>texana</u>	(5)	0.0196 0.0017
<u>turgiceps</u>	(3)	0.0093 0.0016
<u>zebrata</u>	(3)	0.0040 0.0002
<u>zonalis</u>	(3)	0.0032 0.0005

of the mean for body weight (m),  
) , wing length (R), log of wing

AR±SEM	$\rho_W \pm \text{SEM}$ (g/cm <sup>2</sup> )
4.68	
4.38 0.04	0.046 0.004
4.32 0.05	0.048 0.001
3.93 0.08	0.050 0.002
4.52	0.039
4.55	
4.24 0.04	0.048 0.003
4.29 0.03	
4.39	
4.32 0.06	0.043 0.001
4.36 0.04	0.053 0.001
4.26 0.04	0.043 0.003
4.12 0.08	0.042 0.005
4.51 0.04	0.052 0.001
4.30 0.05	0.051 0.008
4.63	
4.96 0.05	0.072 0.002
4.41	0.073
4.15 0.08	0.076 0.019
4.45 0.04	
4.50 0.03	0.054 0.006
4.32 0.12	
4.67 0.07	0.085 0.006
4.39 0.07	0.058 0.010
4.18 0.04	0.032 0.003
4.32 0.02	0.032 0.005

Table 1 (continued).

Genus Species(n)	m±SEM (g)	AR±SEM	P <sub>w</sub> ±SEM (g/cm <sup>2</sup> )
<u>Halictus</u>			
<u>atroviridis</u> (12)	0.0048 0.0006	4.42 0.05	0.052 0.006
<u>hesperus</u> (14)	0.0160 0.0020	4.80 0.02	0.065 0.006
<u>jucundus</u> (5)	0.0118 0.0010	4.92 0.05	0.060 0.003
<u>lineata</u> (3)	0.0089 0.0006	4.71 0.03	0.047 0.002
<u>ligatus</u> (17+24)	0.0374 0.0045	4.93 0.05	0.096 0.007
<u>maculatus</u> (4)	0.0162 0.0016	5.09 0.05	0.062 0.008
<u>parallelus</u> (3)	0.0788 0.0047	5.12 0.02	0.107 0.003
<u>quadrinotus</u> (4)	0.1140 0.0032	5.40 0.04	0.127 0.002
<u>rubicundus</u> (10)	0.0352 0.0028	4.96 0.02	0.075 0.005
<u>sexcinctus</u> (3)	0.0792 0.0079	5.39 0.07	0.108 0.002
<u>Ceratina</u>			
<u>acantha</u> (3)	0.0088 0.0019	4.94 0.03	0.060 0.006
<u>arizonensis</u> (3)	0.0023 0.0003	4.88 0.08	0.047 0.003
<u>asunuionis</u> (3)	0.0345 0.0006	5.34 0.08	0.108 0.008
<u>calcarata</u> (3)	0.0110 0.0009	4.94 0.03	0.067 0.004
<u>chlora</u> (3)	0.0425 0.0002	5.10 0.05	0.123 0.002
<u>cockerelli</u> (5)	0.0027 0.0002	5.12 0.05	0.058 0.003
<u>diodonta</u> (3)	0.0079 0.0021	4.90 0.01	0.077 0.015
<u>dupla</u> (3)	0.0136 0.0010	4.93 0.06	0.083 0.006
<u>hieroglyphica</u> (3)	0.0179 0.0027	5.20 0.02	0.082 0.006
<u>nanula</u> (4)	0.0114 0.0003	4.98 0.09	0.080 0.001
<u>neomexicana</u> (4)	0.0224 0.0058	5.03 0.12	0.101 0.011
<u>pacifica</u> (4)	0.0189 0.0028	5.12 0.09	0.087 0.007
<u>placida</u> (3)	0.0188 0.0019	5.09 0.03	0.093 0.006
<u>rupestris</u> (5)	0.0573 0.0085	5.30 0.03	0.122 0.017
<u>shinnersi</u> (3)	0.0082 0.0012	4.93 0.06	0.083 0.008

Table 1 (continued).

Genus Species(n)	m±SEM (g)
<u>Trigona</u>	
<u>amalthea</u> (3)	0.0645 0.0049
<u>capitata</u> (3)	0.0339 0.0030
<u>duckei</u> complex (4)	0.0023 0.0001
<u>frontalis</u> (3)	0.0047 0.0002
<u>fuscipennis</u> (3)	0.0114 0.0005
<u>latitarsis</u> (3)	0.0036 0.0002
<u>lineata</u> (3)	0.0046 0.0002
<u>mirandula</u> (3)	0.0062 0.0006
<u>pectoralis</u> (3)	0.0135 0.0000
<u>perangulata</u> (3)	0.0135 0.0005
<u>taitara</u> (3)	0.0090 0.0003
<u>testacea</u> (3)	0.0103 0.0009
<u>testaceacornis</u> (3)	0.0069 0.0004
<u>Apis</u>	
<u>cerana</u> (20)	0.0321 0.0025
<u>dorsata</u> (15)	0.0928 0.0022
<u>floreana</u> (20)	0.0177 0.0005
<u>laboriosa</u> (10)	0.1316 0.0063
<u>mellifera</u>	
workers (22)	0.0874 0.0030
queens (10)	0.1229 0.0085
drones (10)	0.1807 0.0045

AR±SEM                      p<sub>w</sub>±SEM (g/cm<sup>2</sup>)

5.27	0.08	0.079	0.006
5.68	0.03	0.092	0.008
4.73	0.07	0.056	0.003
4.79	0.03	0.043	0.002
5.28	0.04	0.051	0.002
5.24	0.06	0.034	0.002
5.12	0.08	0.043	0.003
4.99	0.03	0.040	0.005
5.35	0.02	0.060	0.000
5.62	0.11	0.055	0.001
5.40	0.02	0.043	0.002
5.14	0.05	0.042	0.003
4.97	0.03	0.059	0.003

5.62	0.03	0.080	0.006
6.08	0.03	0.091	0.002
5.74	0.03	0.070	0.002
6.50	0.03	0.116	0.006

5.99	0.03	0.160	0.006
5.70	0.04	0.193	0.012
5.30	0.03	0.169	0.004



Table 1 (continued).

Genus Species(n)	R±SEM (mm)
<u>Perdita</u>	
<u>acapulcona</u> (1)	5.39
<u>albovittata</u> (3)	3.07 0.01
<u>arcuata</u> (3)	3.29 0.10
<u>beameri</u> (3)	3.18 0.06
<u>bequaertiana</u> (1)	7.56
<u>bicolor</u> (1)	5.71
<u>bishoppi</u> (4)	2.70 0.01
<u>californica</u> (2)	4.33 0.24
<u>chihuahua</u> (1)	1.98
<u>coreopsidis</u> (3)	4.30 0.09
<u>cowaniae</u> (3)	4.10 0.06
<u>interrupta</u> (3)	3.61 0.03
<u>lateralis</u> (3)	3.63 0.05
<u>laticauda</u> (3)	2.90 0.06
<u>lingualis</u> (3)	5.03 0.09
<u>maculigera</u> (1)	3.83
<u>maritima</u> (3)	5.64 0.03
<u>mellea</u> (1)	1.97
<u>minima</u> (4)	1.71 0.04
<u>obscuripennis</u> (3)	4.52 0.23
<u>octomaculata</u> (5)	4.33 0.03
<u>portalis</u> (3)	2.73 0.19
<u>texana</u> (5)	5.17 0.08
<u>turgiceps</u> (3)	4.19 0.05
<u>zebrata</u> (3)	3.60 0.06
<u>zonalis</u> (3)	3.30 0.01

log wing area±SEM	log stigma area±SEM
----------------------	------------------------

1.09	-1.12
0.63 0.01	-1.65 0.02
0.70 0.03	-1.66 0.05
0.71 0.03	-1.33 0.01
1.40	-0.56
1.16	-1.29
0.53 0.01	-1.54 0.01
0.94 0.04	-1.41 0.02
0.25	-1.75
0.93 0.01	-1.32 0.01
0.89 0.01	-1.23 0.02
0.79 0.01	-1.29 0.02
0.81 0.003	-1.24 0.03
0.57 0.02	-1.85 0.04
1.07 0.02	-1.17 0.02
0.80	-1.19
1.11 0.01	-1.31 0.03
0.25	-2.11
0.15 0.02	-1.86 0.02
0.96 0.04	-1.27 0.05
0.92 0.01	-1.13 0.02
0.53 0.07	-1.81 0.04
1.06 0.01	-1.39 0.01
0.90 0.01	-1.43 0.03
0.79 0.02	-1.22 0.01
0.70 0.004	-1.38 0.01

Table 1 (continued).

Genus Species (n)	R $\pm$ SEM (mm)
<u>Halictus</u>	
<u>atroviridis</u> (12)	3.19 0.04
<u>hesperus</u> (14)	5.36 0.09
<u>jucundus</u> (5)	4.90 0.14
<u>lineata</u> (3)	4.72 0.05
<u>ligatus</u> (17+24)	6.69 0.29
<u>maculatus</u> (4)	5.78 0.10
<u>parallelus</u> (3)	9.97 0.13
<u>quadricinctus</u> (4)	10.96 0.18
<u>rubicundus</u> (10)	7.62 0.08
<u>sexcinctus</u> (3)	9.93 0.48
<u>Ceratina</u>	
<u>acantha</u> (3)	4.20 0.24
<u>arizonensis</u> (3)	2.43 0.09
<u>asunuionis</u> (3)	6.56 0.25
<u>calcarata</u> (3)	4.50 0.09
<u>chlora</u> (3)	6.64 0.09
<u>cockerelli</u> (5)	2.42 0.08
<u>diodonta</u> (3)	3.46 0.21
<u>dupla</u> (3)	4.50 0.02
<u>hieroglyphica</u> (3)	5.29 0.21
<u>nanula</u> (4)	4.21 0.08
<u>neomexicana</u> (4)	5.14 0.54
<u>pacifica</u> (4)	5.24 0.23
<u>placida</u> (3)	5.08 0.15
<u>rupestris</u> (5)	7.86 0.16
<u>shinnersi</u> (3)	3.47 0.09

log wing area±SEM	log stigma area±SEM
----------------------	------------------------

0.66 0.01	-1.50 0.01
1.08 0.02	-1.12 0.02
0.99 0.02	-1.28 0.02
0.98 0.01	-1.25 0.02
1.25 0.04	-1.05 0.03
1.12 0.02	-1.06 0.02
1.56 0.01	-0.74 0.02
1.56 0.02	-0.65 0.04
1.37 0.01	-0.89 0.02
1.56 0.04	-0.69 0.05

0.85 0.05	-1.19 0.04
0.38 0.04	-1.66 0.05
1.21 0.03	-1.07 0.05
0.91 0.02	-1.25 0.02
1.24 0.01	-0.97 0.02
0.36 0.04	-1.65 0.02
0.69 0.05	-1.31 0.04
0.91 0.003	-1.17 0.01
1.03 0.03	-1.08 0.04
0.85 0.01	-1.24 0.01
1.01 0.09	-1.14 0.07
1.03 0.04	-1.11 0.03
1.01 0.02	-1.18 0.03
1.37 0.02	-0.94 0.06
0.69 0.03	-1.38 0.03

Table 1 (continued).

Genus Species(n)	R±SEM (mm)
<u>Trigona</u>	
<u>amalthea</u> (3)	10.38 0.07
<u>capitata</u> (3)	7.24 0.03
<u>duckei</u> complex (4)	2.21 0.10
<u>frontalis</u> (3)	3.64 0.03
<u>fuscipennis</u> (3)	5.42 0.08
<u>latitarsis</u> (3)	3.70 0.01
<u>lineata</u> (3)	3.74 0.20
<u>mirandula</u> (3)	4.42 0.08
<u>pectoralis</u> (3)	5.50 0.02
<u>perangulata</u> (3)	5.89 0.06
<u>taitara</u> (3)	5.30 0.06
<u>testacea</u> (3)	5.60 0.06
<u>testaceicornis</u> (3)	3.83 0.02
<u>Apis</u>	
<u>cerana</u> (20)	7.50 0.03
<u>dorsata</u> (6)	12.48 0.08
<u>florea</u> (20)	6.05 0.02
<u>laboriosa</u> (10)	13.53 0.08
<u>mellifera</u>	
workers (22)	9.06 0.03
queens (10)	9.52 0.07
drones (10)	11.92 0.11

log wing area±SEM	log stigma area±SEM
----------------------	------------------------

1.61 0.01	-0.61 0.02
1.27 0.004	-1.06 0.01
0.31 0.03	-1.55 0.02
0.74 0.01	-1.30 0.03
1.05 0.01	-1.12 0.02
0.72 0.01	-1.28 0.01
0.73 0.04	-1.36 0.03
0.89 0.02	-1.17 0.01
1.05 0.003	-1.24 0.03
1.09 0.01	-1.11 0.003
1.02 0.01	-1.16 0.02
1.09 0.005	-1.07 0.01
0.77 0.004	-1.40 0.01

1.30 0.004	-1.53 0.01
1.71 0.004	-1.09 0.02
1.11 0.002	-1.30 0.01
1.75 0.005	-1.19 0.02

1.44 0.003	-1.50 0.02
1.50 0.01	-1.34 0.02
1.73 0.01	-1.55 0.03

Table 2. Allometric equations for the relationship between stigma area ( $S_S/2$ ) and total wing area ( $S/2$ ) for one wing pair. P values indicate the probability of rejecting the null hypothesis of isometry (an exponent equal to 1.0).

Halictus (n=10)

$$S_S/2 = -2.09 (S/2)^{0.878} \quad p < 0.001$$

Perdita (n=26)

$$S_S/2 = -2.12 (S/2)^{0.911} \quad p < 0.5 \quad \text{ns}$$

Ceratina (n=15)

$$S_S/2 = -1.88 (S/2)^{0.723} \quad p < < 0.001$$

Trigona (n=13)

$$S_S/2 = -1.83 (S/2)^{0.674} \quad p < 0.001$$

Apis (n=5)

$$S_S/2 = -1.93 (S/2)^{0.420} \quad p < 0.02 \quad \text{ns}$$

Halictus ligatus (n=41)

$$S_S/2 = -2.09 (S/2)^{0.824} \quad p < 0.001$$

Table 3. Elements of the first unit eigen vector of the forewing principal components analysis for each group. Allometric trends shared by all or most groups are indicated in the right-most column (+, ++ = positive, strongly positive allometry; -, -- = negative, strongly negative allometry).

	<u>Perdita</u>	<u>Halictus</u>	<u>Ceratina</u>	<u>Trigona</u>	<u>Apis</u>	<u>Halictus ligatus</u>	
R-1	.159	.174	.174	.231	.171	.160	
R-2	.143	.141	.132	.078	.229	.139	-
R-3	.155	.184	.184	.279	.160	.165	
R-4	.157	.167	.170	.198	.159	.156	
Cu1-1	.136	.140	.153	.170	.128	.154	-
Cu1-2	.157	.171	.165	.209	.155	.160	
Marg-1	.188	.168	.183	.216	.167	.158	+
Marg-2	.106	.153	.167	.113	.150	.167	-
SM1-1	.157	.169	.161	.153	.117	.167	
SM1-2	.136	.171	.119	.208	.155	.162	
SM1-3	.175	.168	.183	.122	.175	.169	
SM2-1	.473	.220	.266		.141	.239	++
SM2-2	.161	.174	.140		.186	.178	
SM2-3	.192	.167	.157		.170	.172	
SM3-1		.168	.213		.228	.135	+
SM3-2		.169	.163	.219	.138	.174	
SM3-3		.196	.185		.166	.176	+
D-1	.134	.141	.128	.204	.140	.127	-
D-2	.103	.153	.123	.133	.146	.163	-
D-3	.108	.141	.099	.188	.162	.156	--



Table 3 (continued).

	<u>Perdita</u>	<u>Halictus</u>	<u>Ceratina</u>
M1-1	.177	.182	.186
M1-2	.145	.142	.136
M1-3	.176	.168	.178
M1-4	.172	.168	.202
M1-5	.164	.177	.162
M2-1	.177	.183	.190
M2-2	.157	.157	.149
M2-3	.186	.199	.157
M2-4	.143	.147	.143
M2-5	.208	.195	.208
M2-6	.132	.156	.184
D-4	.175	.152	.144
D-5	.088	.143	.112
D-6	.149	.153	.154
Cu2-1	.147	.149	.169
Cu2-2	.147	.160	.154
H <sub>0</sub> :	.174	.167	.167
% variance explained:	89.7	97.9	96.4

<u>Trigona</u>	<u>Apis</u>	<u>Halictus</u> <u>ligatus</u>	
.236	.176	.179	+
.196	.171	.163	-
.185	.181	.181	
.219	.167	.189	
.226	.176	.170	
	.175	.178	+
	.146	.146	-
	.175	.158	
	.198	.178	
	.152	.169	+
.195	.157	.144	
.193	.152	.175	
.209	.181	.161	--
.199	.176	.178	
.197	.147	.153	-
.206	.175	.165	
.196	.167	.167	
94.3	94.5	95.3	

Table 4. Elements of the first unit eigen vector of the hindwing principal components analysis for each group. Allometric trends shared by all or most groups are indicated in the right-most column (+, ++ = positive, strongly positive allometry; -, -- = negative, strongly negative allometry).

	<u>Perdita</u>	<u>Halictus</u>	<u>Ceratina</u>	<u>Trigona</u>	<u>Apis</u>	<u>Halictus</u> <u>ligatus</u>	
R-1	.257	.252	.216	.295	.256	.242	
R-2	.233	.286	.309	.258	.297	.299	+
R-3	.234	.228	.260		.178	.174	-
R-4	.251	.268	.294	.336	.297	.307	++
R-5	.241	.270	.219		.240	.255	
R-6	.265	.259	.238		.292	.240	
R-5+6				.276			
R-7	.223	.210	.204	.271	.202	.213	--
Cu1-1	.273	.217	.233		.218	.230	-
Cu1-2	.270	.256	.232		.291	.253	

Table 4 (continued).

	<u>Perdita</u>	<u>Halictus</u>
D-1	.221	.231
D-2	.225	.221
D-3	.238	.225
D-4	.235	.221
D-5		
D-6	.217	.224
D-7	.244	.253
D-6+7		
D-8	.237	.259
D-9	.250	.226
H <sub>0</sub> :	.243	.243
% variance explained:	91.7	96.7

<u>Ceratina</u>	<u>Trigona</u>	<u>Apis</u>	<u>Halictus</u> <u>ligatus</u>	
.205	.304	.251	.248	-
.248			.241	-
.227	.375	.297	.237	
.241	.285	.215	.206	-
	.222			-
.105			.169	--
.360			.283	
	.269	.217		-
.230	.320	.250	.246	
.208	.212	.321	.235	
.243	.289	.258	.243	
95.5	94.2	93.2	89.9	

Table 5. Mean wing length ( $R'$ ), aspect ratio ( $AR'$ ) and non-dimensional radius of first moment of wing area ( $r_1$ ) and the standard errors of the mean for diverse hymenopteran groups. Sample sizes, when greater than one, are given in parentheses.

taxon	$R' \pm \text{SEM}$ (mm)	$AR' \pm \text{SEM}$	$r_1 \pm \text{SEM}$
Ichneumonidae:			
<u>Megaryhyssa macrurus</u>	28.21	9.52	.478
<u>Acrodactyla quadrisculpta</u>	5.81	6.53	.491
<u>Zaglyptus varipes</u>	4.21	6.49	.507
<u>Zatypoda nigriceps</u>	3.72	6.10	.481
<u>Adelognathus</u> sp.	3.60	5.00	.473
<u>Orthocentrus</u> sp. (2)	2.96 0.08	5.06 0.16	.481 0.003
Braconidae:			
<u>Macrocentrus</u> sp. (2)	9.74 0.08	5.92 0.01	.498 0.002
<u>Apanteles nephrotericis</u> (2)	2.73 0.05	4.79 0.09	.467 0.0003
<u>Cotesia congregatus</u> (2)	2.38 0.01	4.72 0.01	.469 0.004
<u>Praon</u> sp.	2.70	5.67	.517
Chalcidoidea:			
Leucospidae sp. (1)	7.53	6.48	.491
Leucospidae sp. (2)	8.80 0.24	6.89 0.02	.477 0.006
Pteromalidae sp. (2)	1.40 0.09	5.22 0.19	.508 0.009
<u>Aprostocetus</u> sp.	1.88	5.88	.559
<u>Aprostocetus</u> sp.	1.54	7.73	.565
Tetrastichini sp. (2)	1.15 0.01	5.91 0.12	.546 0.003
Cynpoidea:			
<u>Ibalia maculipennis</u>	13.11	7.80	.478
<u>Alloxysta</u> sp.	1.42	6.52	.543
<u>Alloxysta</u> sp.	2.08	6.18	.537

## Table 5 (continued).

taxon

Pompilidae:

Pepsis thisbe (2)Priocnemis germana

Sphecoidea:

Ectemnius 10-maculatus (2)Crabro latipesBelomicrus viereckiCerceris frontataC. finitimaPsen punctatusPluto sp.Pulverro mescalero (2)Ammoplanops cockerelli (2)Sphecius speciosusClytemnestra sp. (2)Didineis sp.

Apoidea:

Ptiliglossa quianaCaupolicana hirsutuEuryglossa intermediaE. flaviventris

R' ± SEM	AR' ± SEM	r <sub>1</sub> ± SEM
32.10 0.7	5.82 0.02	.441 0.000
7.27	6.39	.483
9.77 1.08	7.95 0.11	.487 0.0004
7.41	7.48	.490
2.60	6.32	.477
18.33	6.78	.474
4.74	6.23	.492
7.60	6.51	.480
5.10	6.01	.486
2.38 0.02	5.14 0.07	.485 0.002
1.59 0.01	4.96 0.14	.487 0.003
27.00	6.31	.459
5.31 0.23	6.59 0.11	.486 0.002
4.97	6.10	.495
13.32	5.70	.442
12.60	5.57	.430
2.24	4.51	.454
2.04	4.46	.453



Table 5 (continued).

taxon

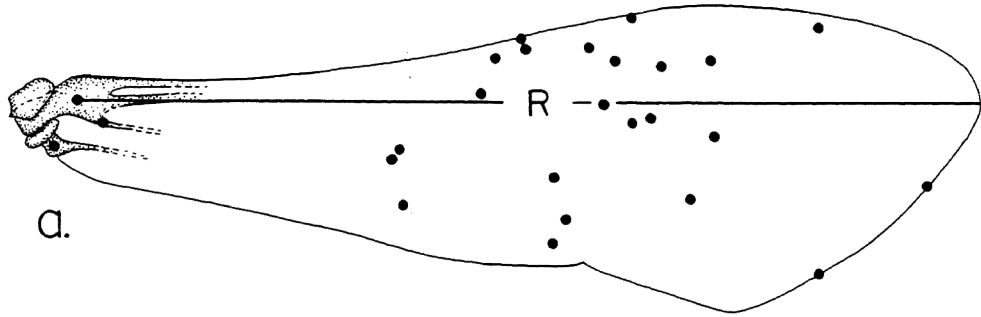
Perdita bequaertianaP. maritima (3)P. chihuahuaP. minima (2)Halictus quadricinctus (3)H. atroviridis (3)Thalestria sp. (2)Triepeolus remigatusNeolarra californicaCeratina rupestris (3)C. cockerelli (3)Trigona amalthea (4)T. duckei (3)Apis laboriosa (3)A. mellifera (5 workers)A. mellifera (5 workers)\*A. florea (3)

\* From Ellington, 1984

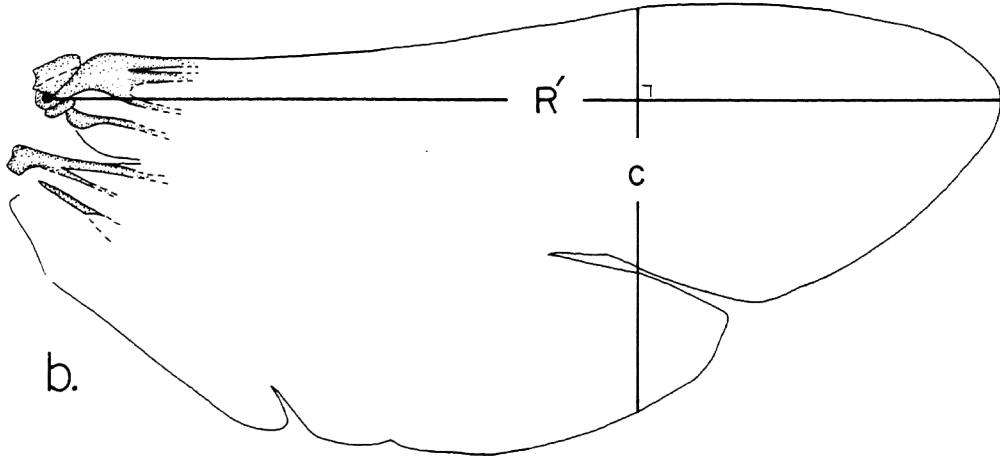
R' ±SEM	AR' ±SEM	r <sub>1</sub> ±SEM
8.08	5.06	.464
6.06 0.04	5.72 0.02	.462 0.003
2.08	4.90	.460
1.80 0.08	4.75 0.07	.473 0.006
11.68 0.12	5.96 0.10	.465 0.0002
3.32 0.14	5.21 0.003	.455 0.001
11.44 0.24	6.02 0.08	.476 0.004
11.08	6.24	.480
2.28	5.64	.488
8.44 0.25	5.98 0.04	.465 0.003
2.47 0.06	5.63 0.05	.480 0.002
10.98 0.05	5.90 0.06	.482 0.002
2.27 0.01	5.30 0.05	.475 0.001
14.03 0.07	7.05 0.02	.488 0.002
9.55 0.05	6.51 0.09	.485 0.002
9.52 0.19	6.65 0.07	.480 0.002
6.36 0.08	6.24 0.10	.473 0.001

Figure 1. Two types of coordinate files (R, R', wing length; c, wing chord).

- a. Coordinate file type 1.
- b. Coordinate file type 2.



a.



b.

Figure 2. Regression of log stigma area on log wing area. A - e show mean values for each species (open circles indicate greater than one point). See Table 1 for actual values. A slope of 1.0 is isometry.

- a. Perdita (P. beq. = P. bequaertiana)
- b. Halictus
- c. Ceratina
- d. Trigona
- e. Apis (queens and drones, although shown on the graph, were not used in calculation of the regression equation)
- f. Halictus ligatus intraspecific allometry

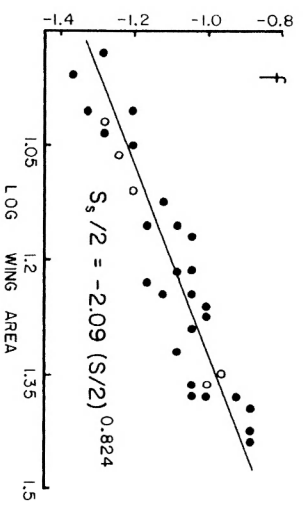
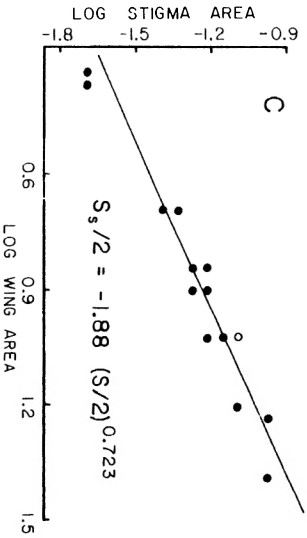
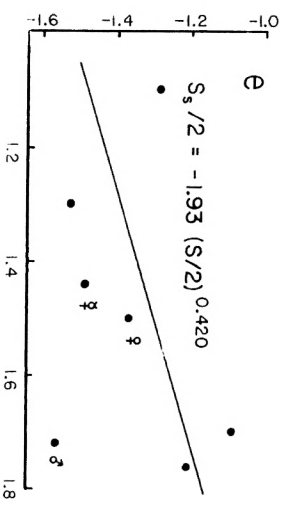
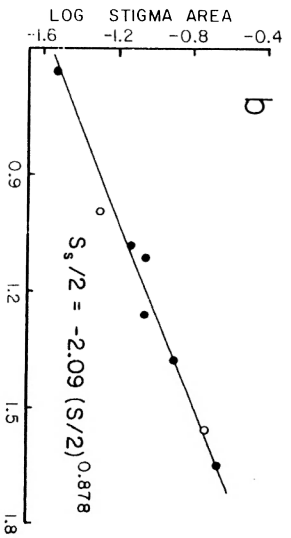
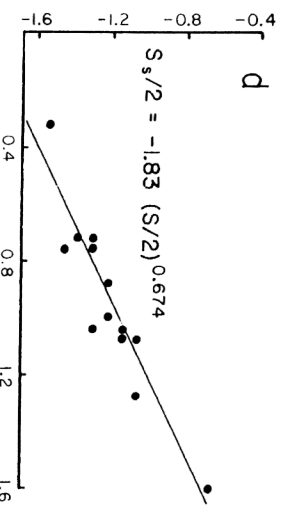
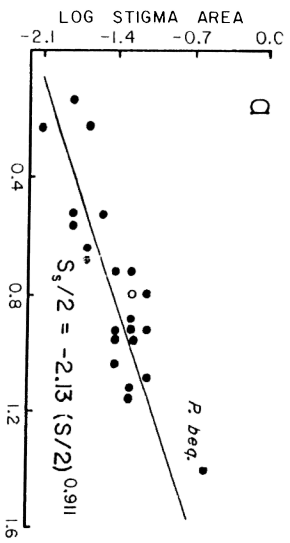


Figure 3. Ichneumonidae (Scale bars in Figs. 3-17 represent 1.0mm except where indicated; position of aerodynamic center indicated by point.)

a. Megarhyssa macrurus

b. Orthocentrus sp.

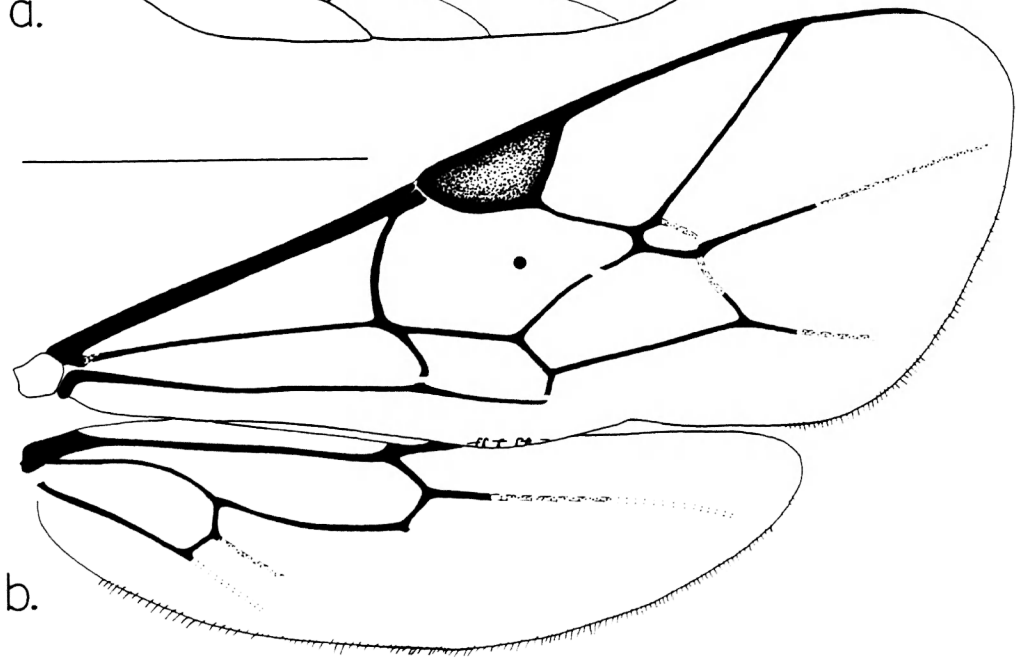
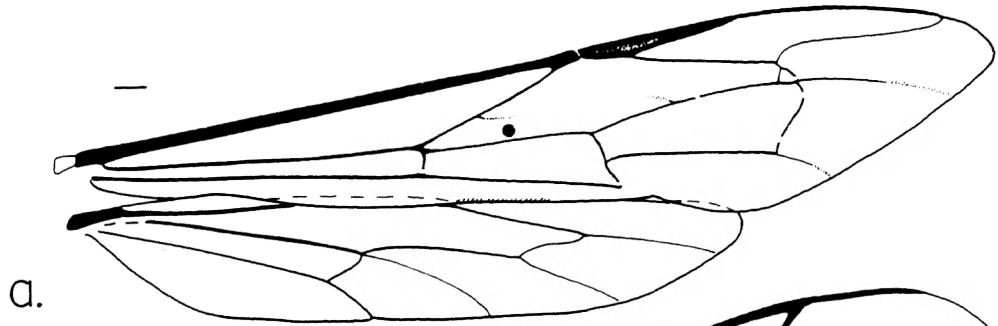




Figure 4. Braconidae, Praon sp.

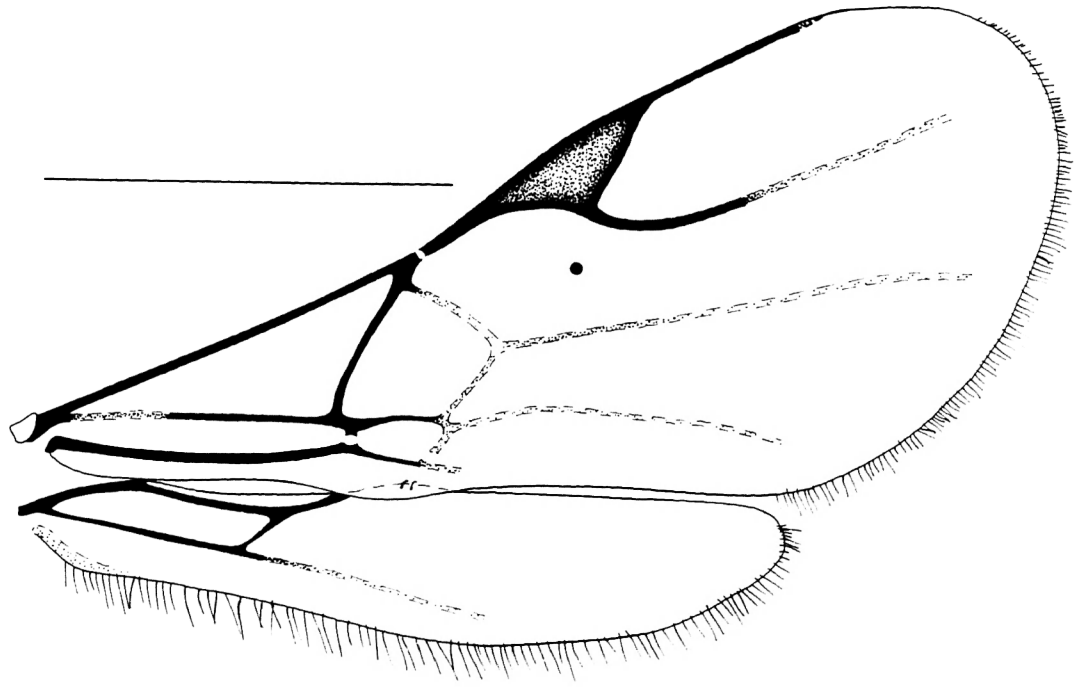
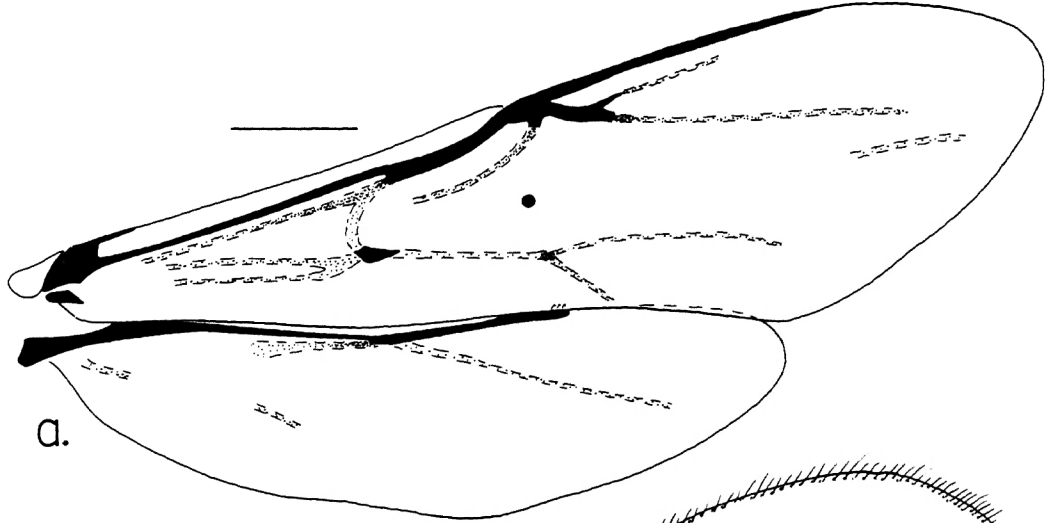
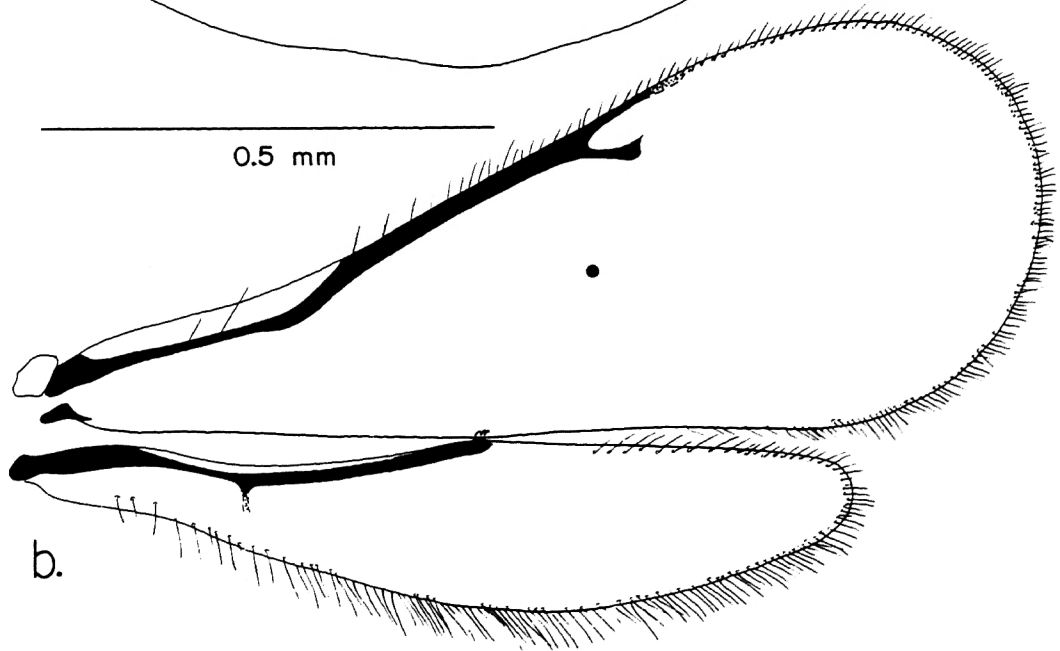


Figure 5. Chalcidoidea

- a. Leucospis affinis, Leucospidae
- b. Tetrastichini sp., Pteromalidae



d.



0.5 mm

b.

Figure 6. Cynipoidea

- a. Ibalia maculipennis, Ibalidae
- b. Alloxysta sp., Cynipidae

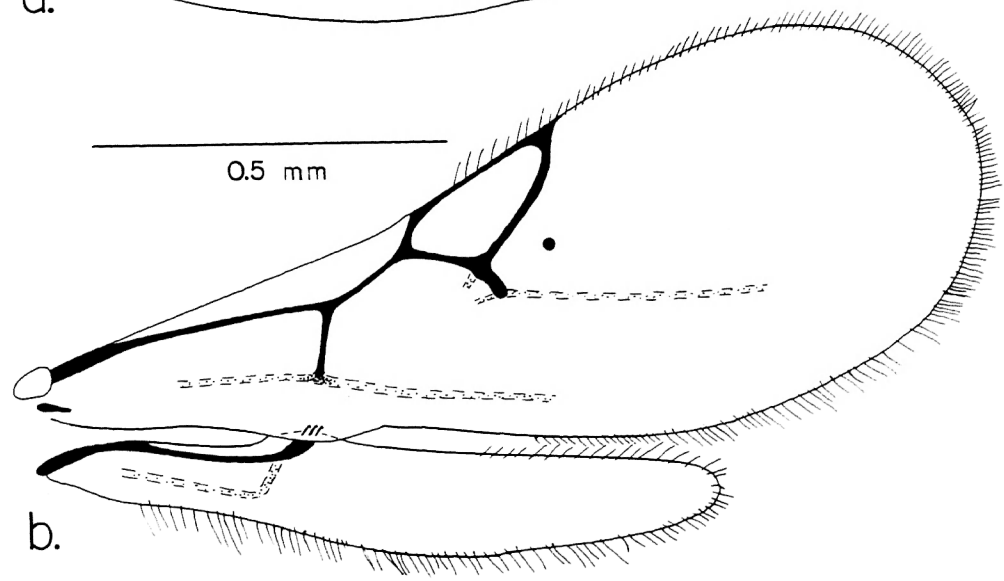
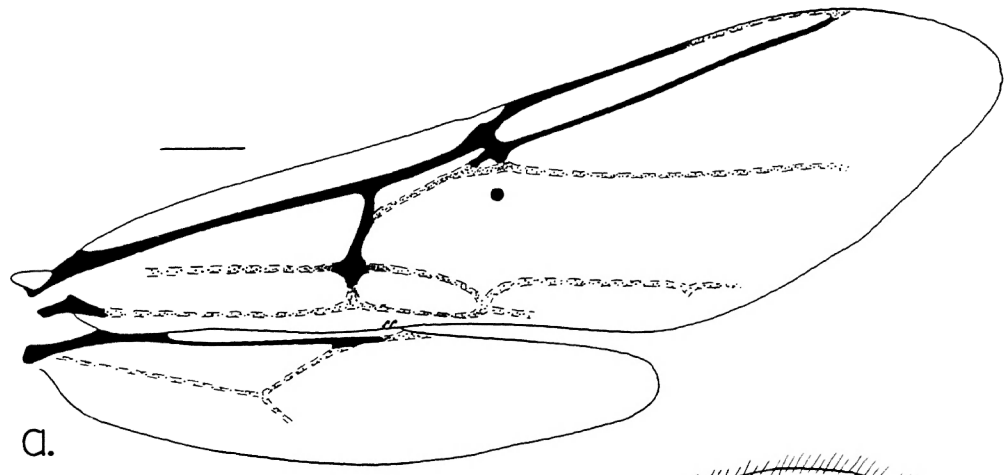


Figure 7. Pompilidae, Pepsis thisbe

Figure 8. Sphecidae: Nyssoninae, Sphecius speciosus

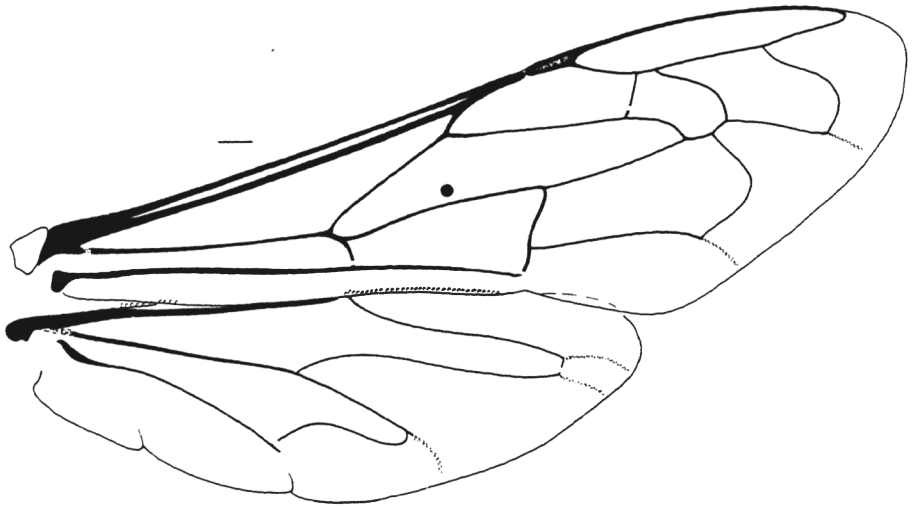
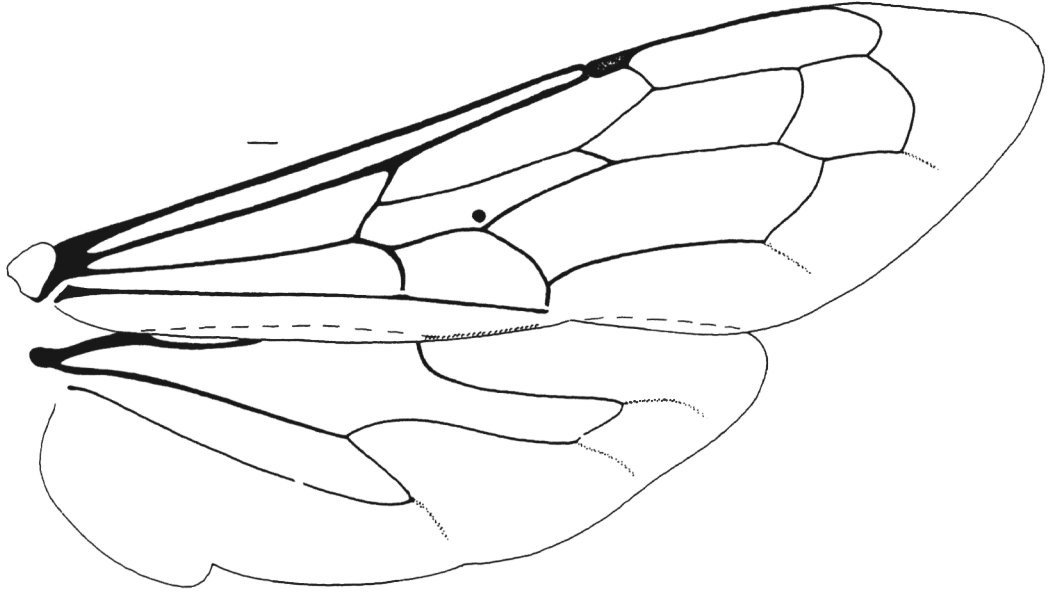




Figure 9. Sphecidae: Pemphredoninae

a. Psen punctatus

b. Ammoplanops cockerelli

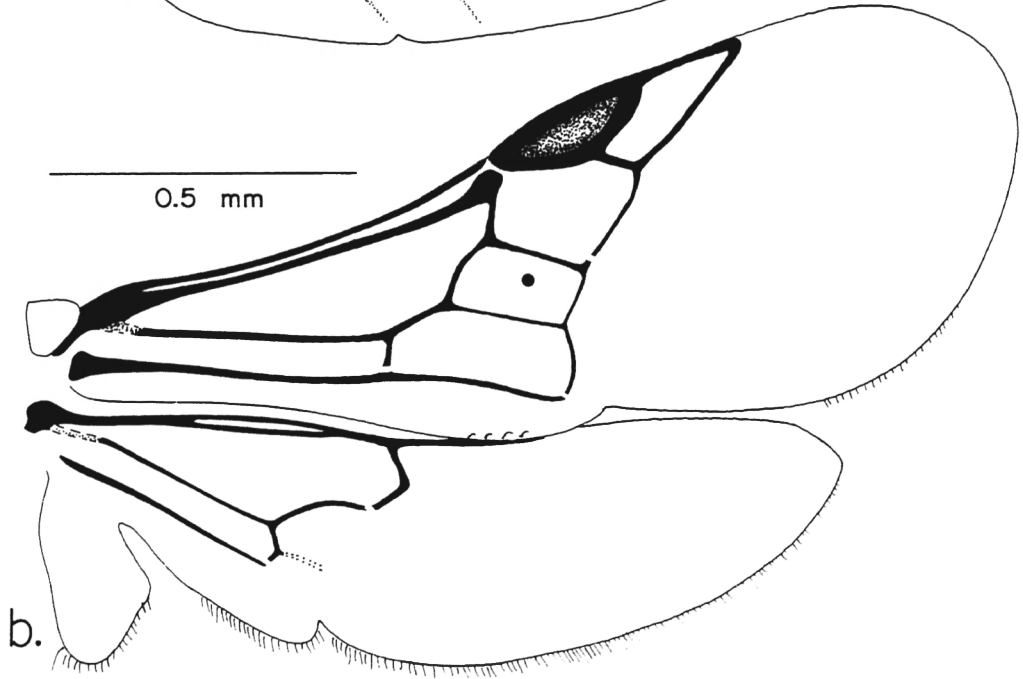
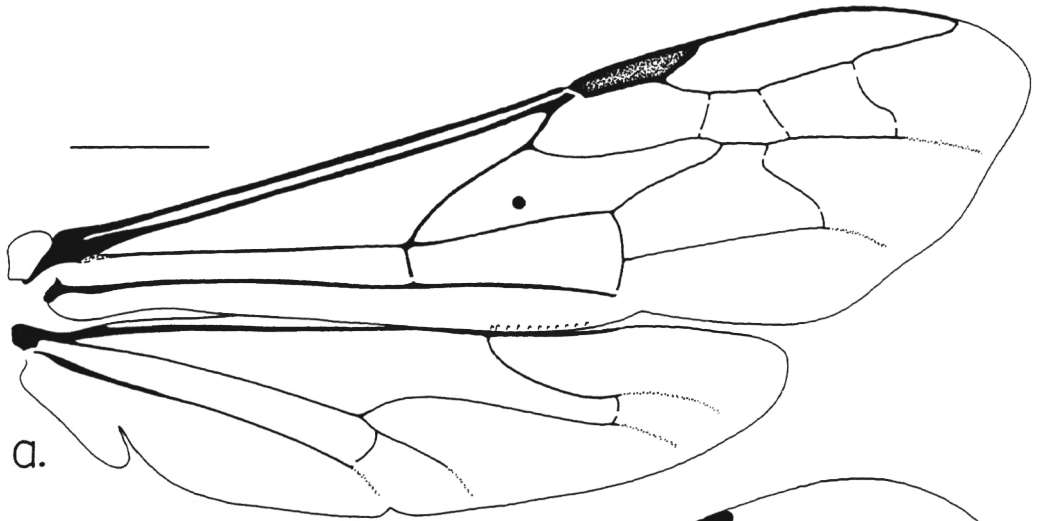


Figure 10. Sphecidae: Crabroninae

a. Ectemnius 10-maculatus

b. Belomicrus vierecki

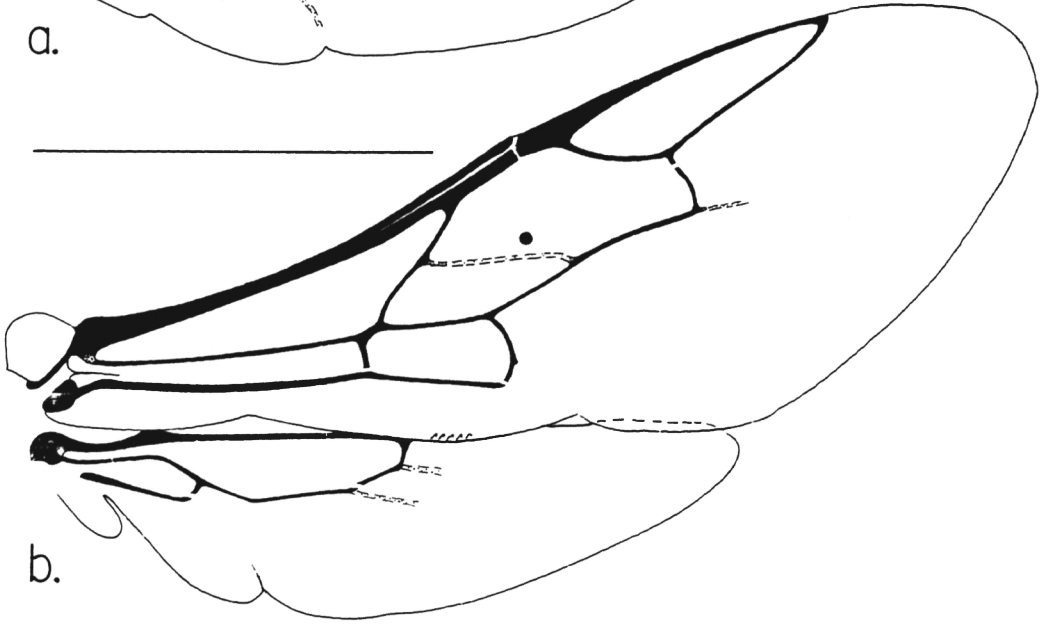
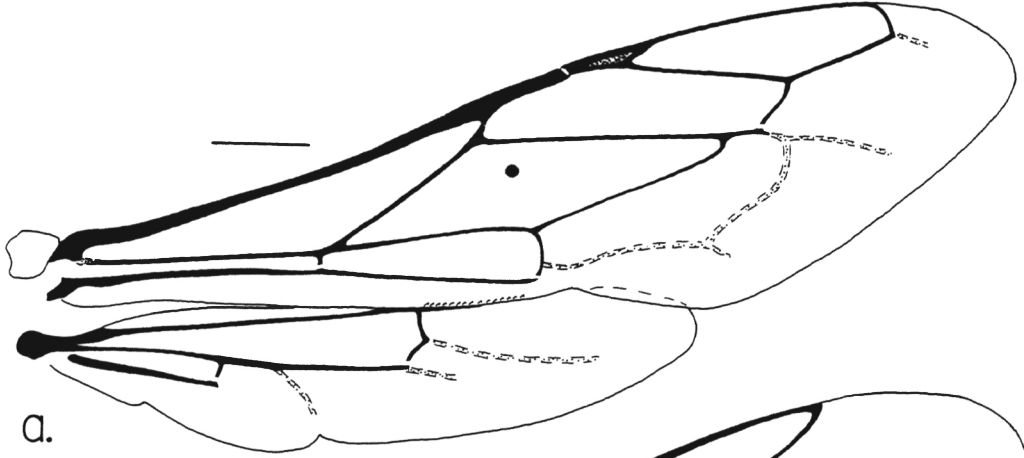


Figure 11. Colletidae

- a. Ptiliglossa quiana
- b. Euryglossa intermedia

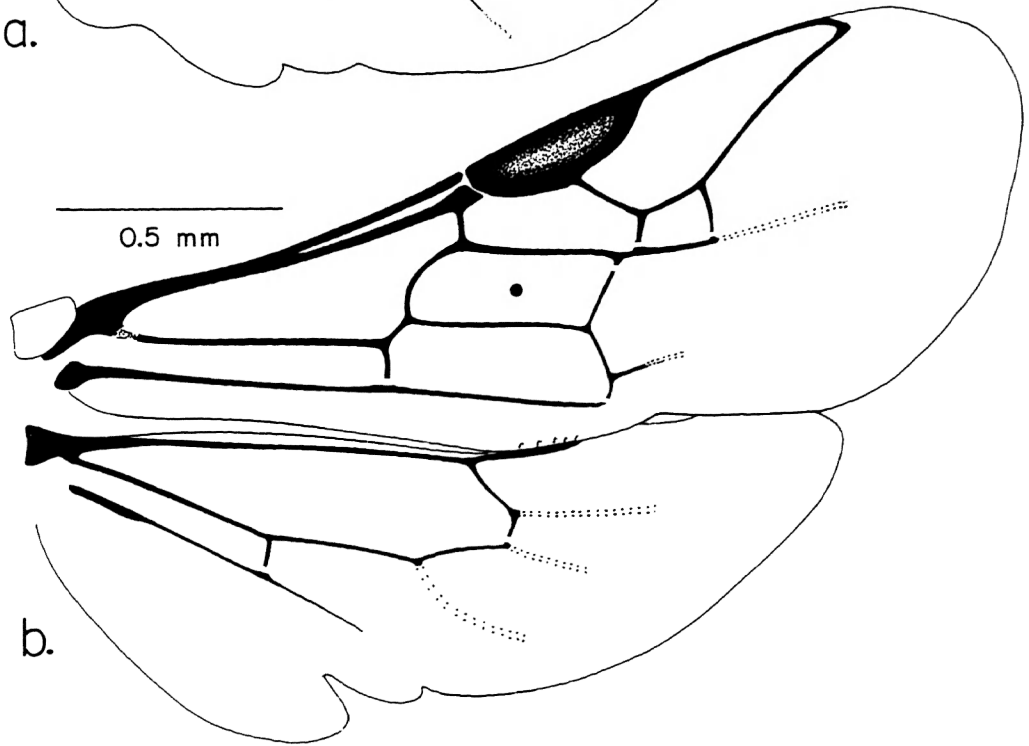
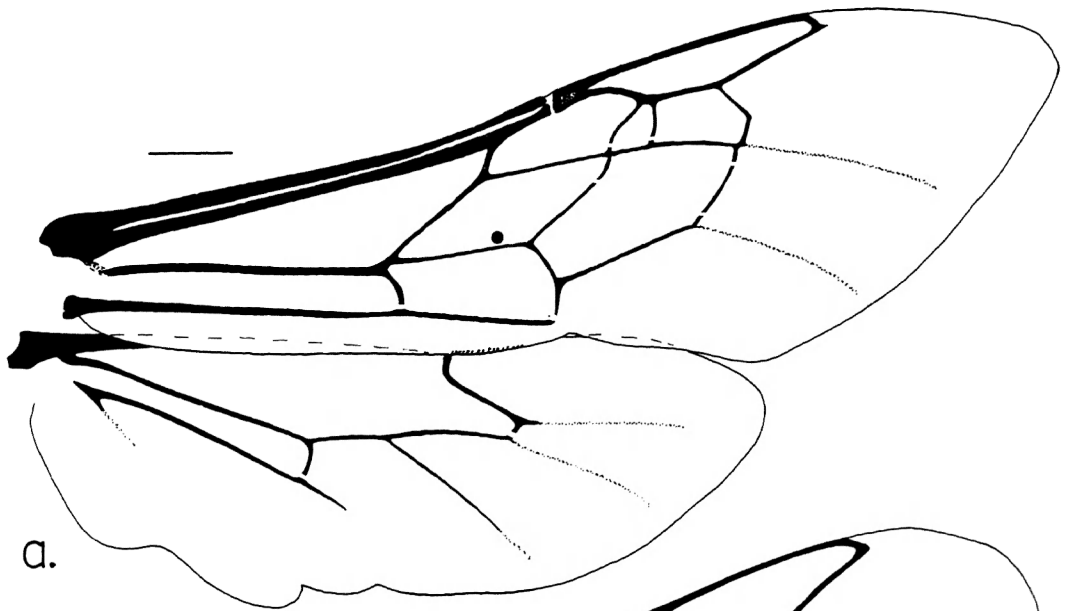


Figure 12. Andrenidae

- a. Perdita texana
- b. P. minima
- c. P. bequaertiana

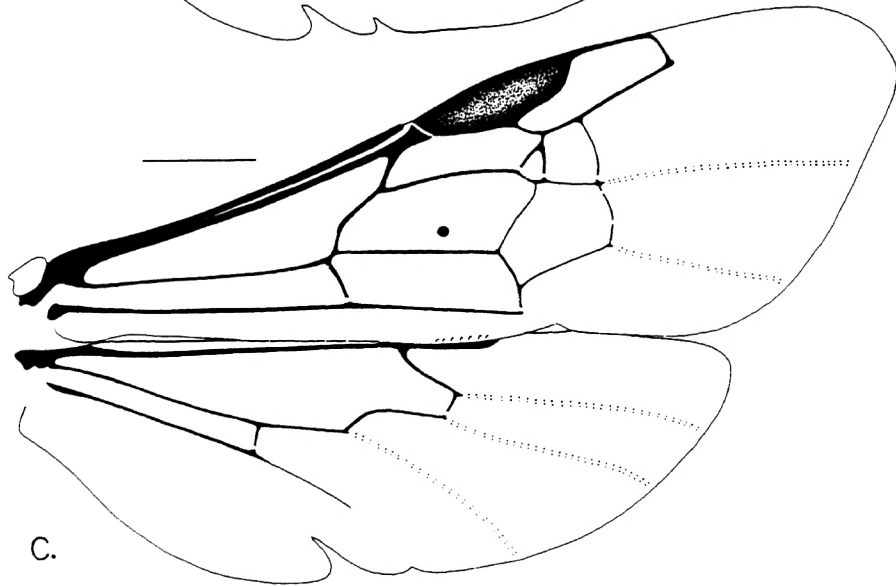
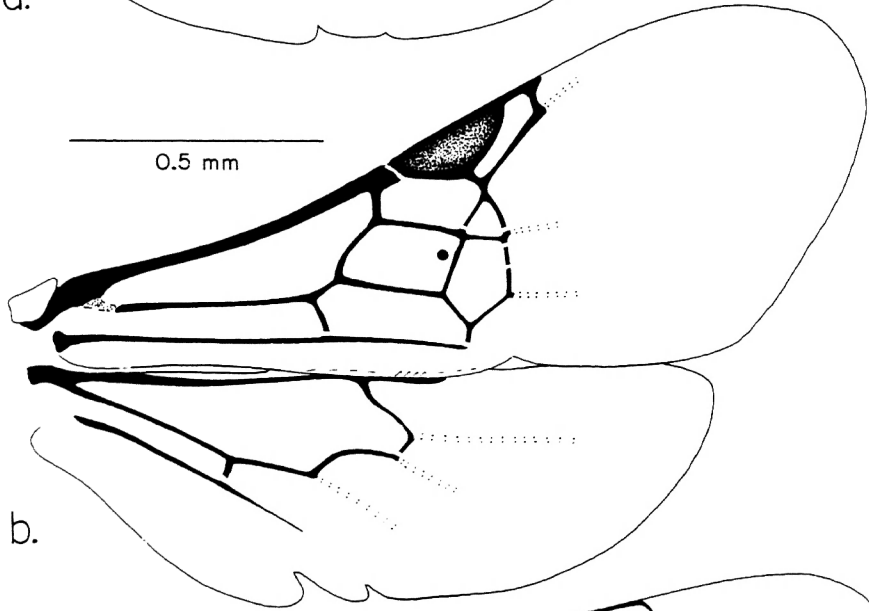
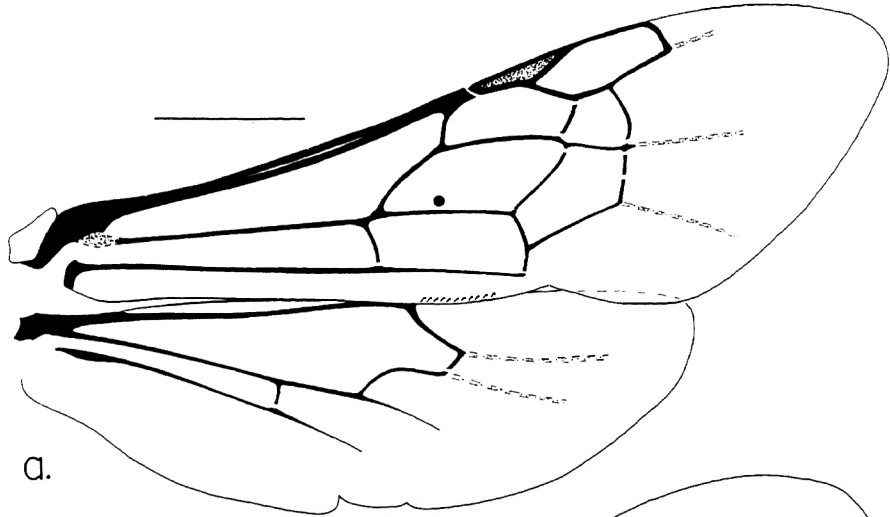




Figure 13. Halictidae

a. Halictus quadricinctus

b. H. atroviridis

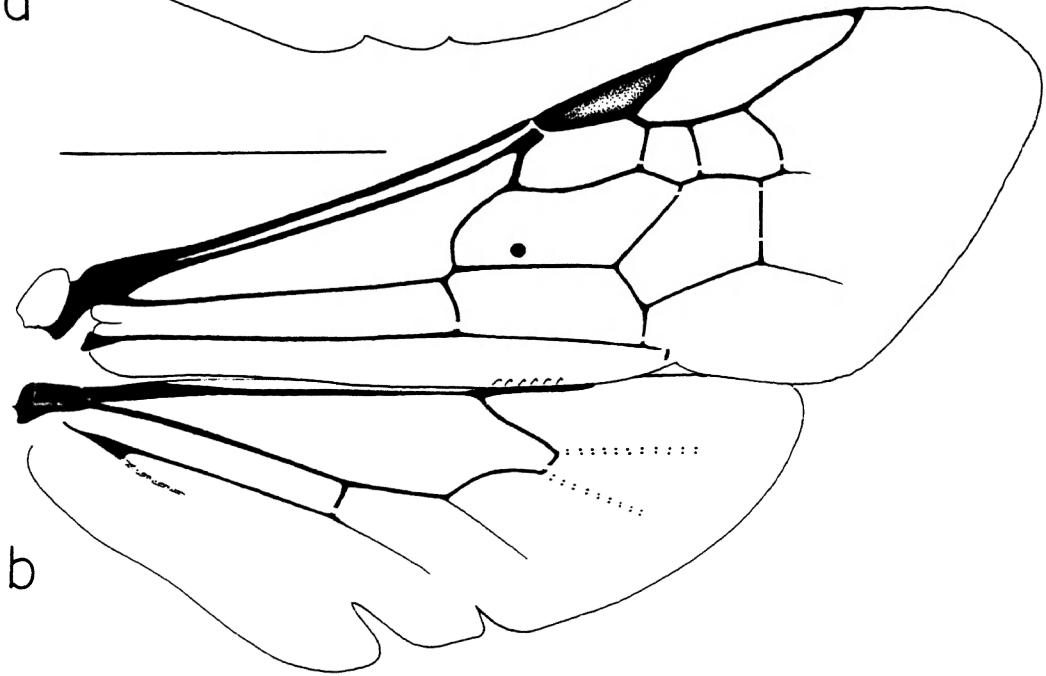
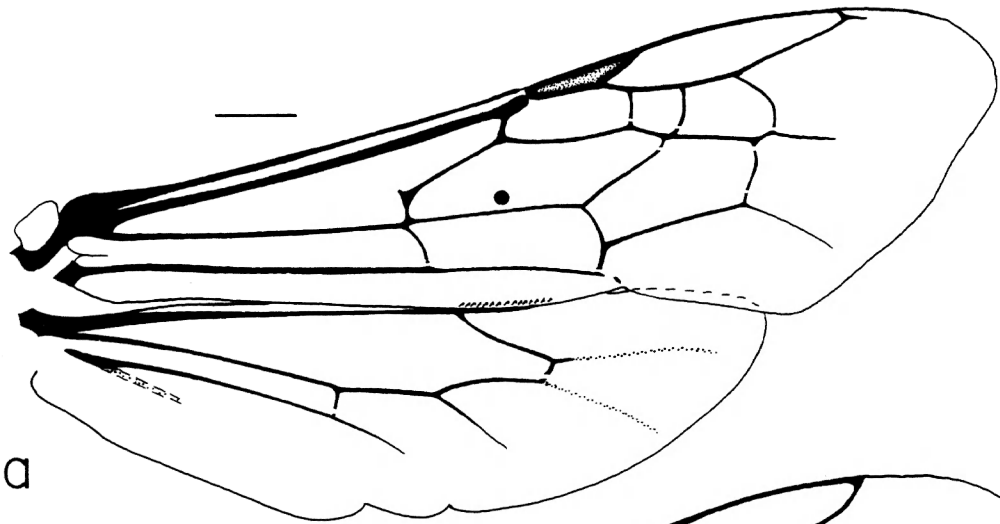


Figure 14. Anthophoridae

a. Ceratina rupestris

b. C. cockerelli

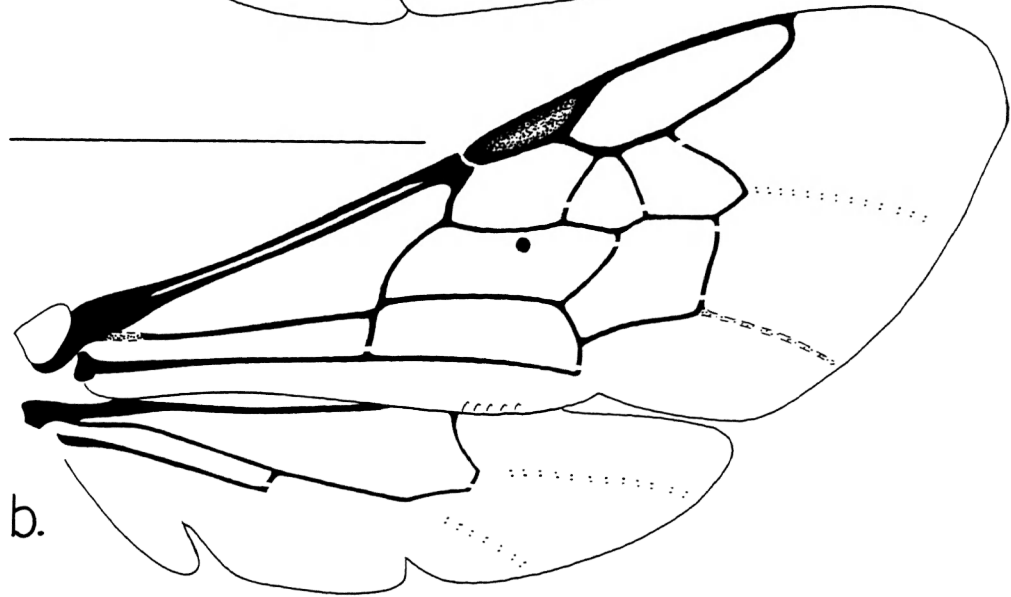
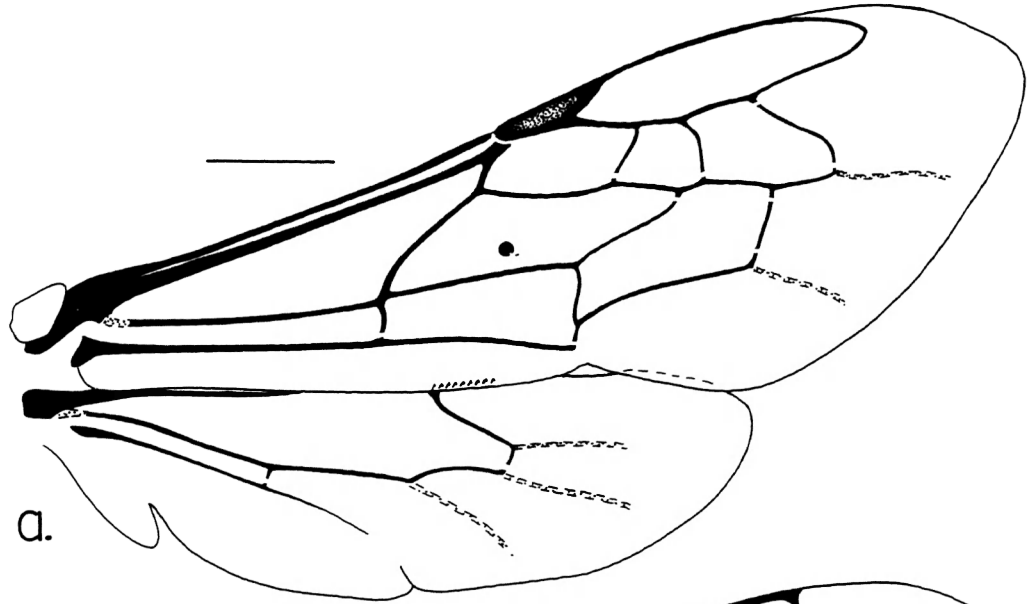


Figure 15. Anthophoridae

a. Thalestria sp.

b. Neolarra californica

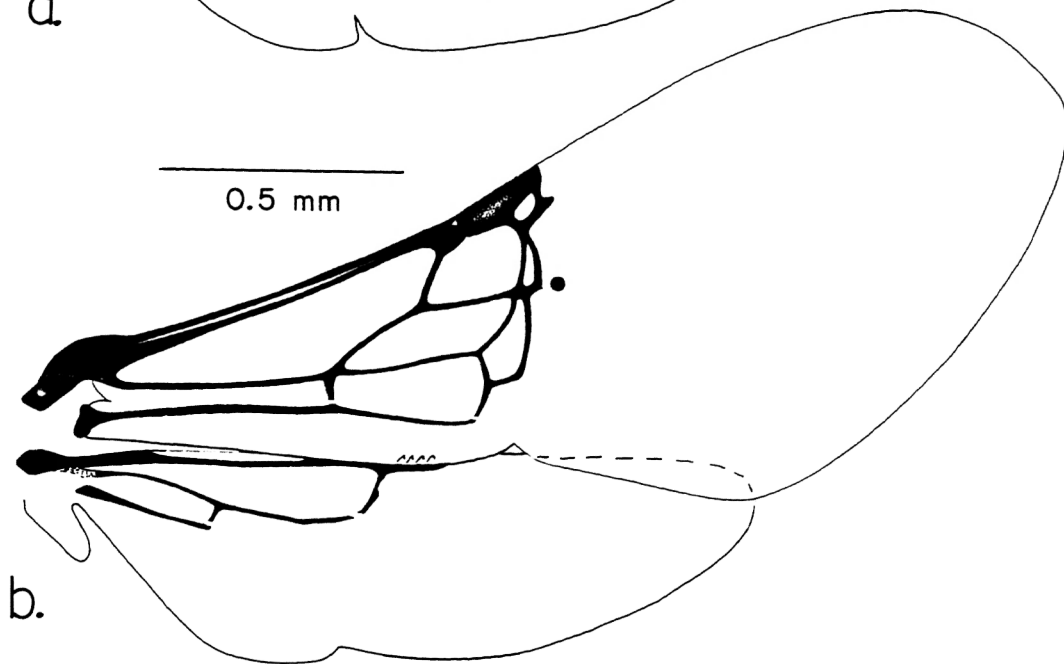
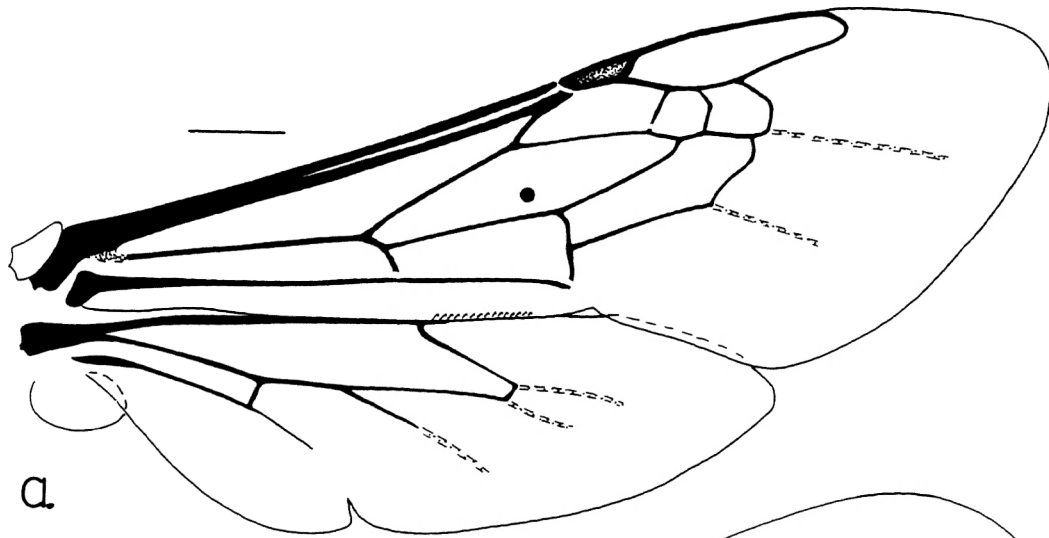


Figure 16. Apidae: Meliponini

a. Trigona amalthea

b. T. duckei

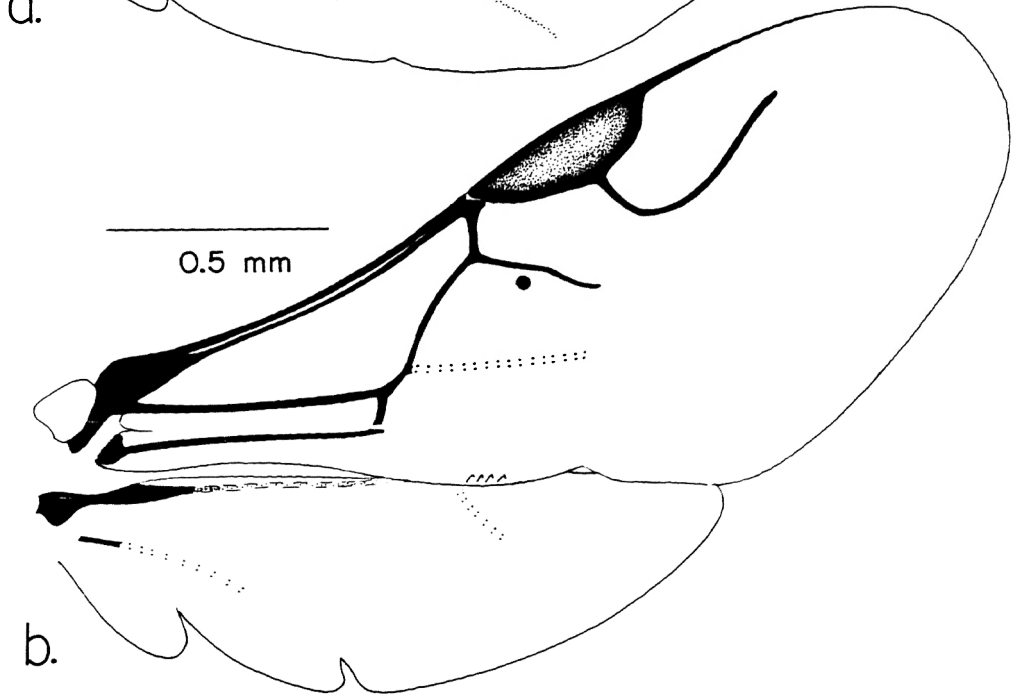
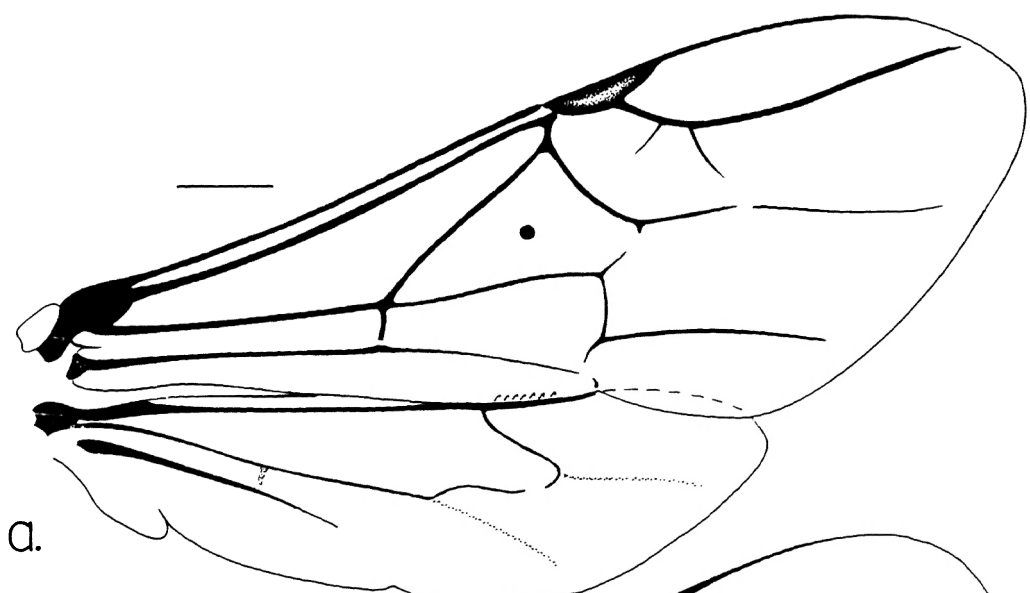




Figure 17. Apidae: Apini

a. Apis laboriosa

b. A. florea

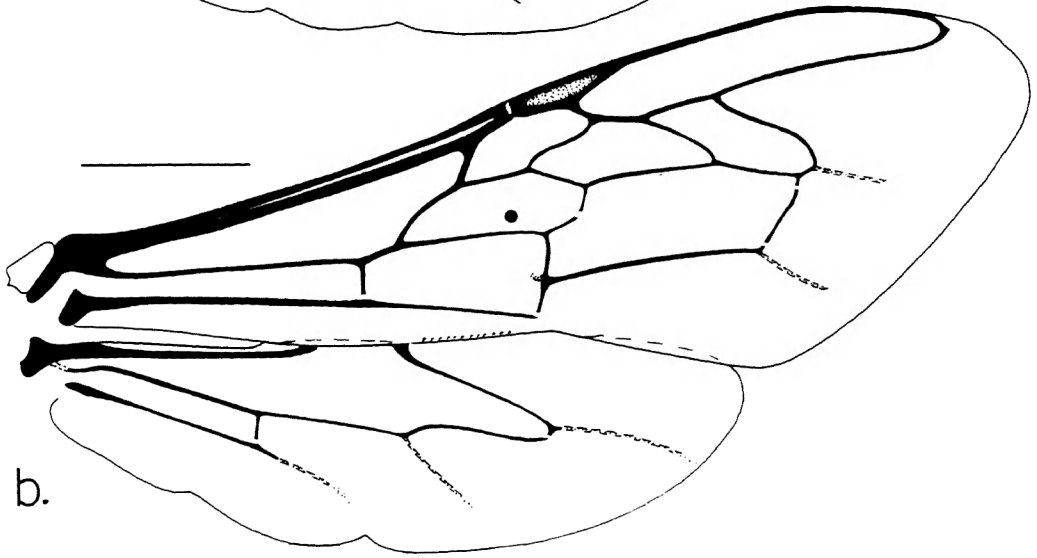
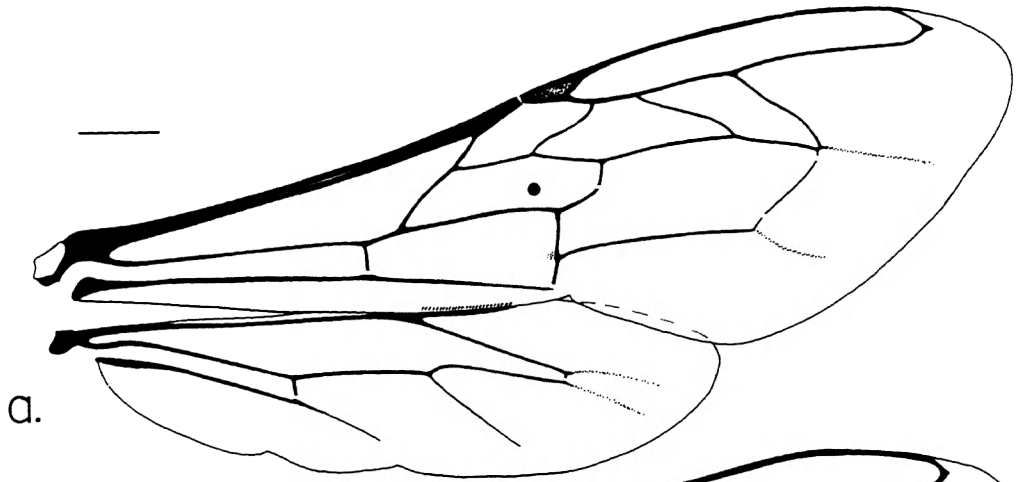


Figure 18. Ceratina rupestris fore and hind wings illustrating wing vein and cell terminology used in text.

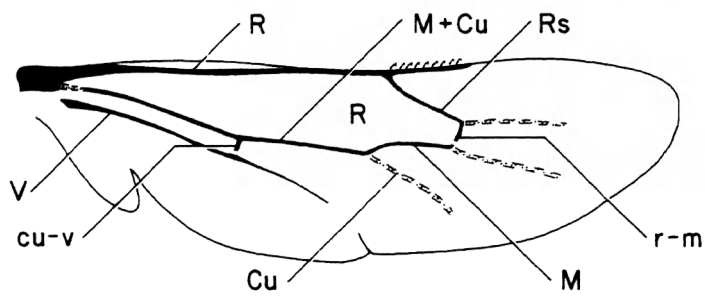
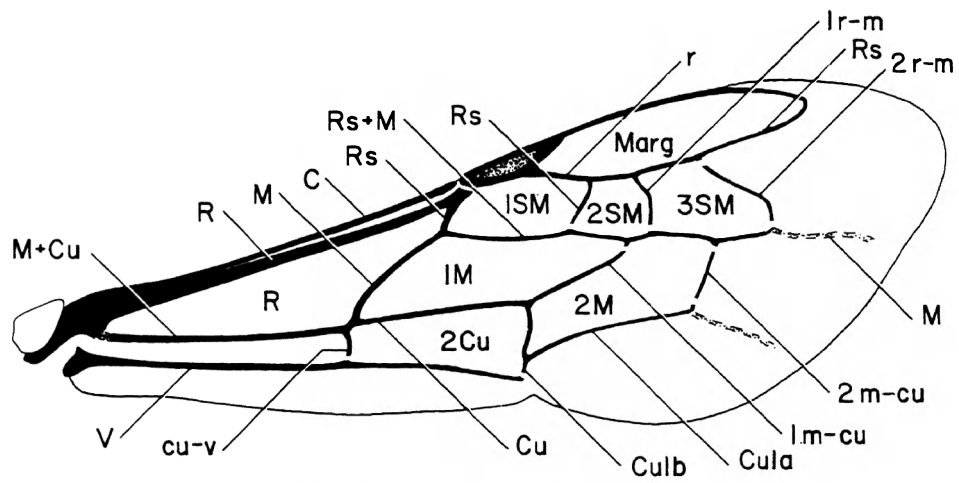


Figure 19. Diagrammatic fore and hind wings illustrating variables used in multivariate morphometric analysis.

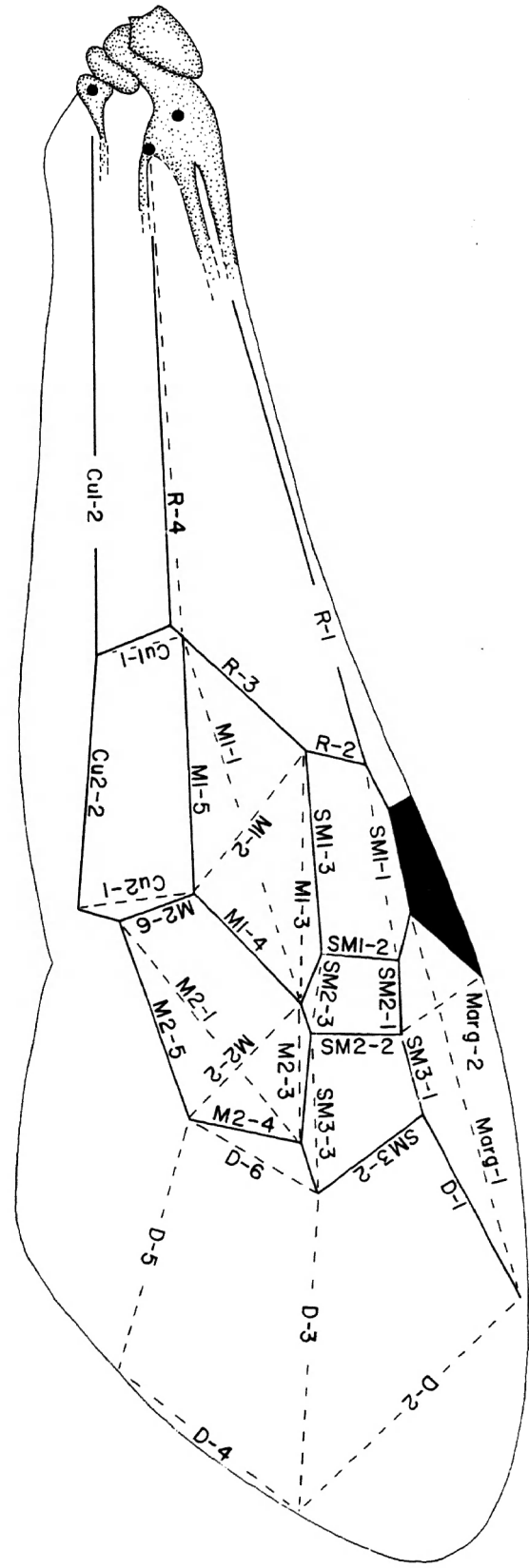
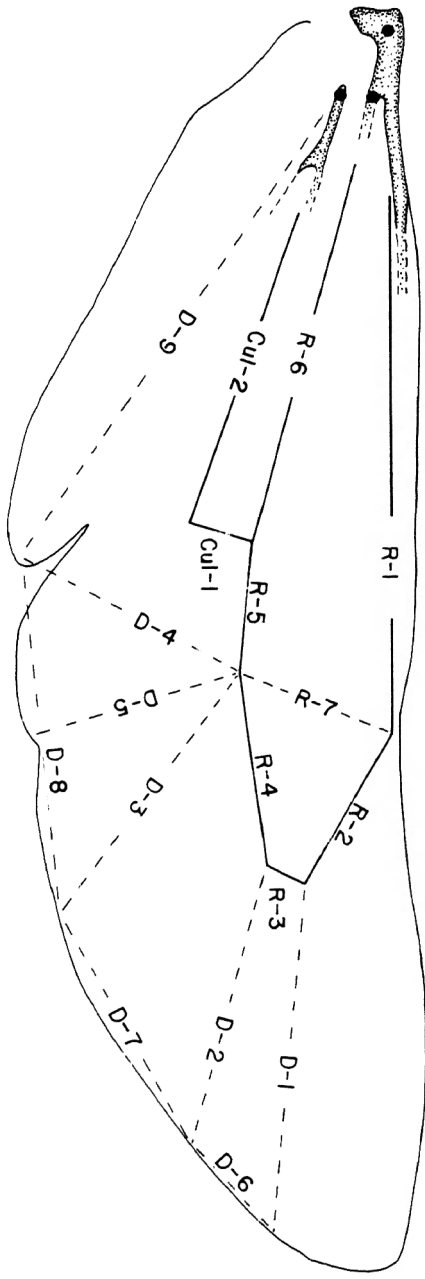


Figure 20. Diagrammatic fore and hind wings illustrating vein pattern changes associated with increase in size. Reversal of arrows would indicate changes associated with decreasing size.

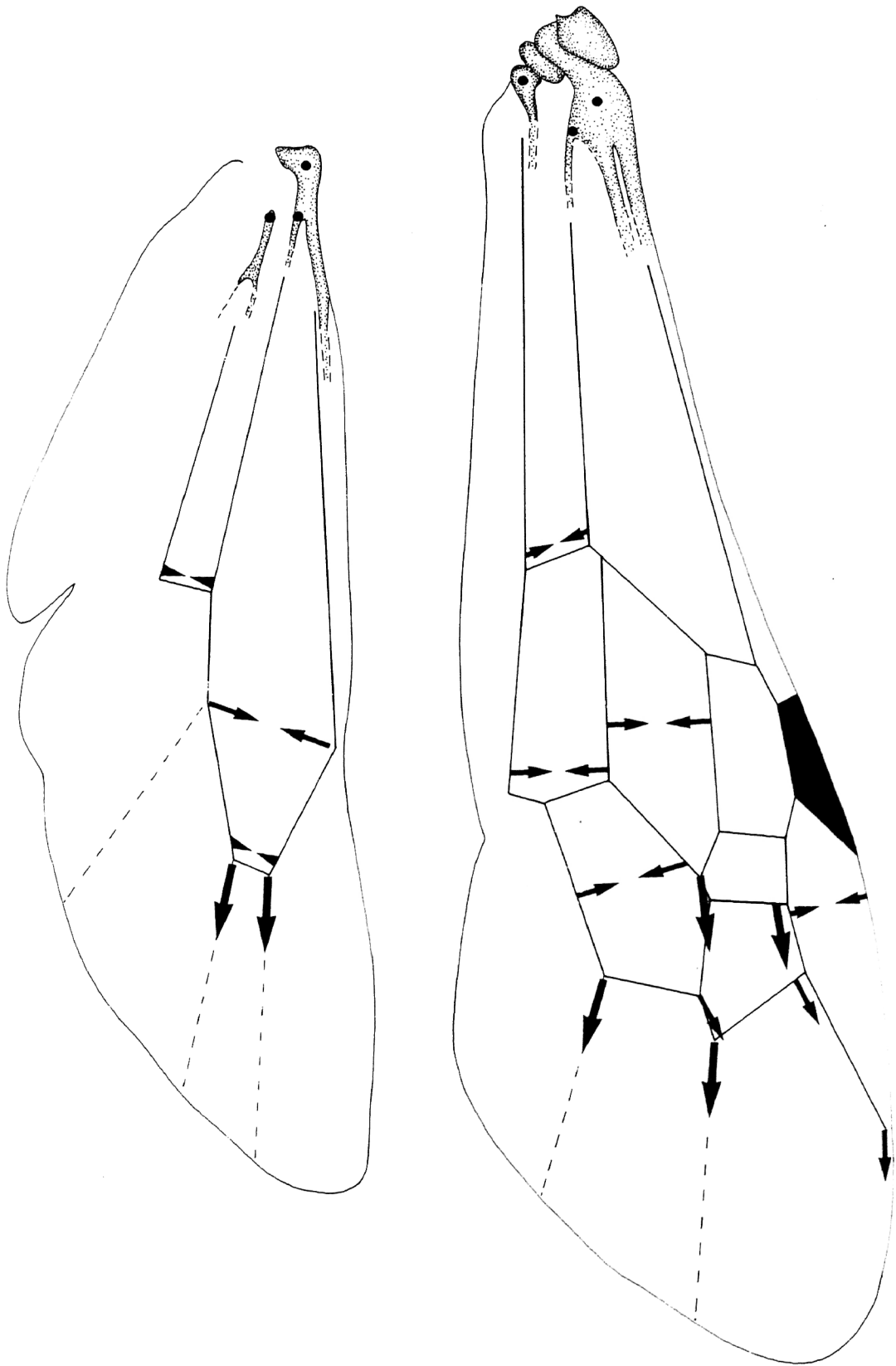




Figure 21. Relationship between aspect ratio on body weight. A - e show mean values for each species (open circles indicate greater than one point). See Table 1 for actual values.

- a. Perdita (P. beq = P. bequaertiana)
- b. Halictus
- c. Ceratina
- d. Trigona
- e. Apis
- f. Halictus ligatus intraspecific allometry

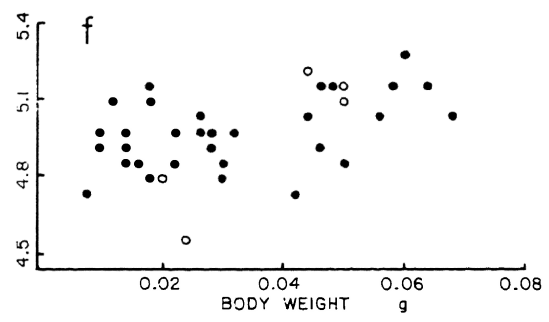
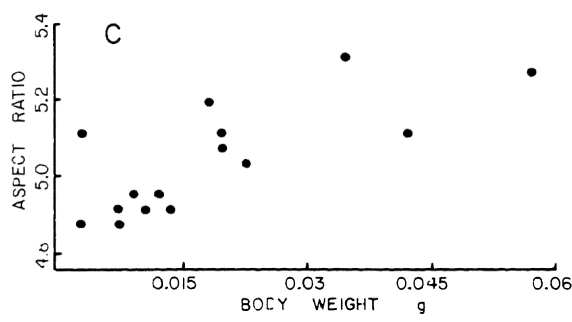
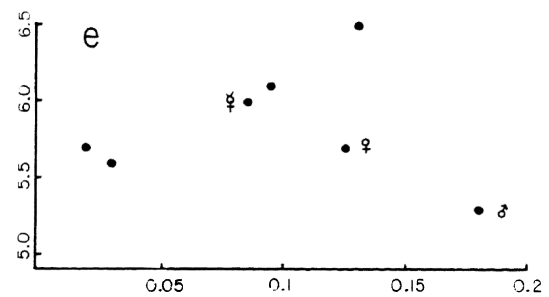
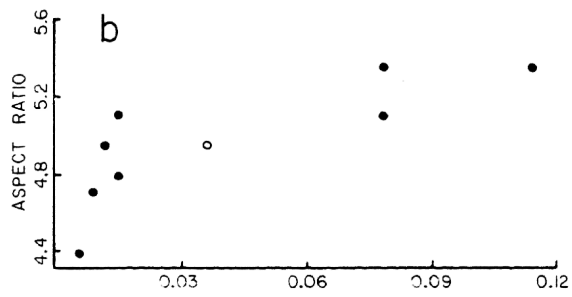
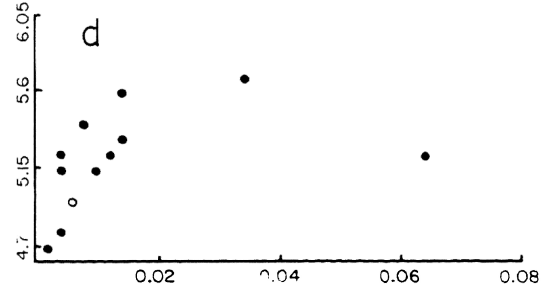
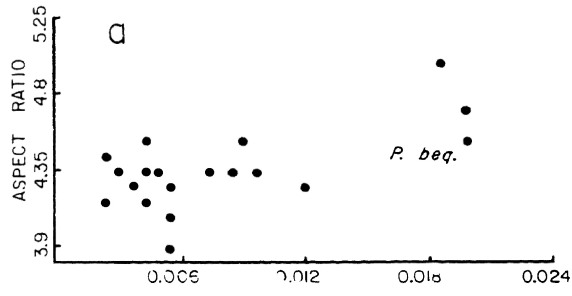


Figure 22. Relationship between non-dimensional radius of the centroid of wing area ( $r_1$ ) and wing length ( $R'$ ) for taxa listed in Table 5. (Open circles indicate more than one point.)

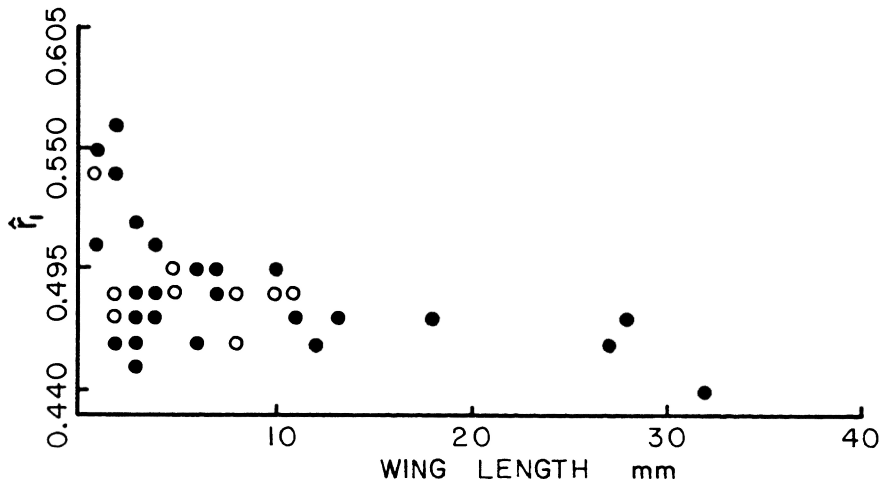


Figure 23. Relationship between wing loading and body weight. A - e show mean values for each species (open circles indicate greater than one point). See Table 1 for actual values.

- a. Perdita (P.beq = P. bequaertiana)
- b. Halictus
- c. Ceratina
- d. Trigona
- e. Apis
- f. Halictus ligatus intraspecific allometry

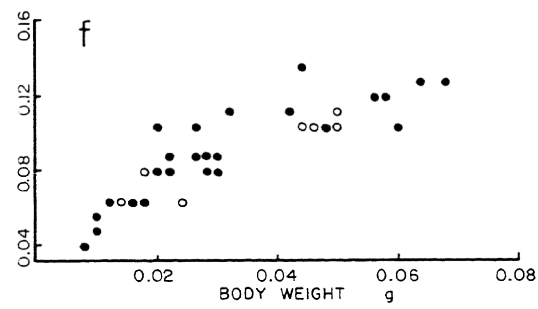
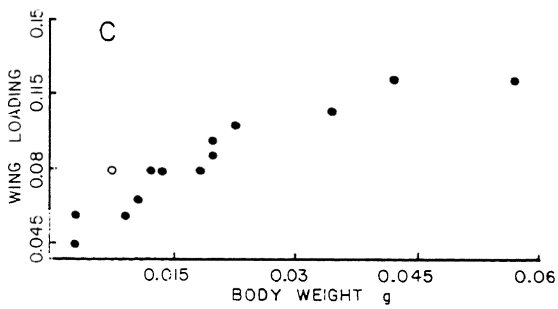
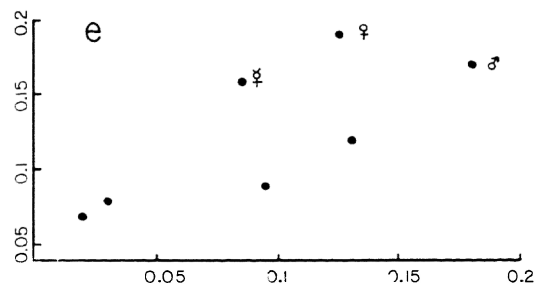
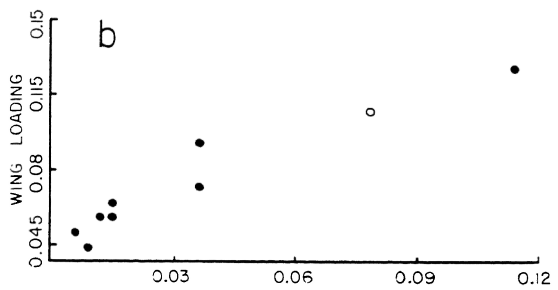
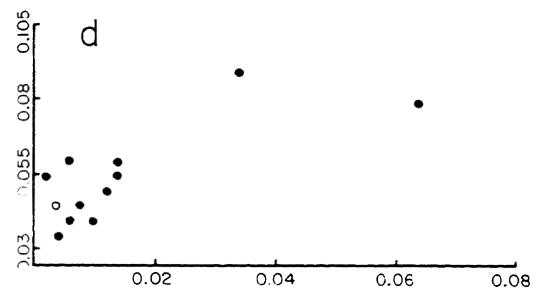
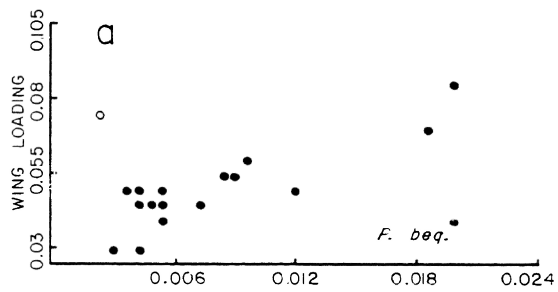
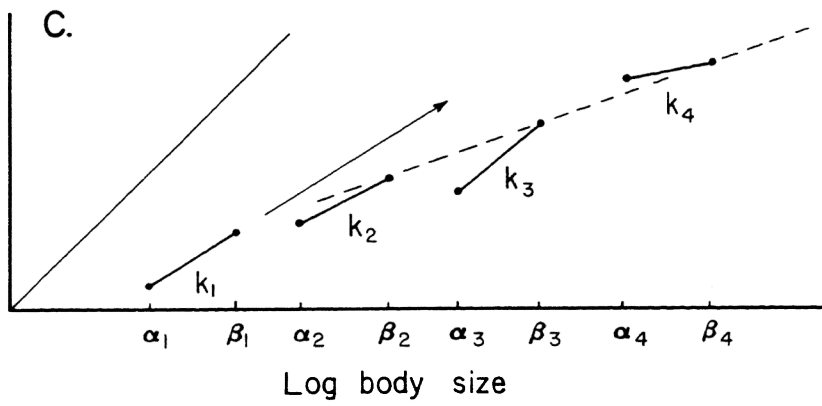
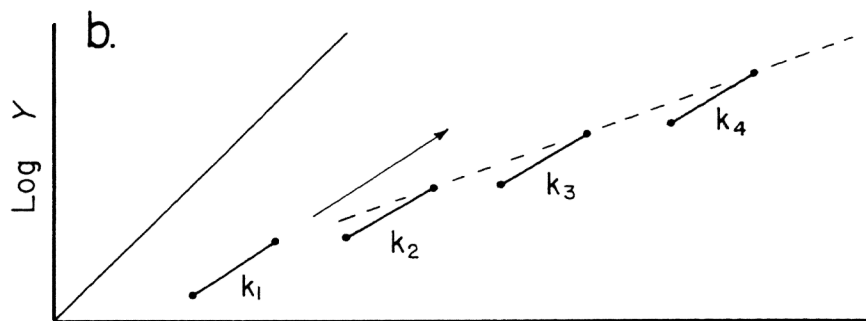
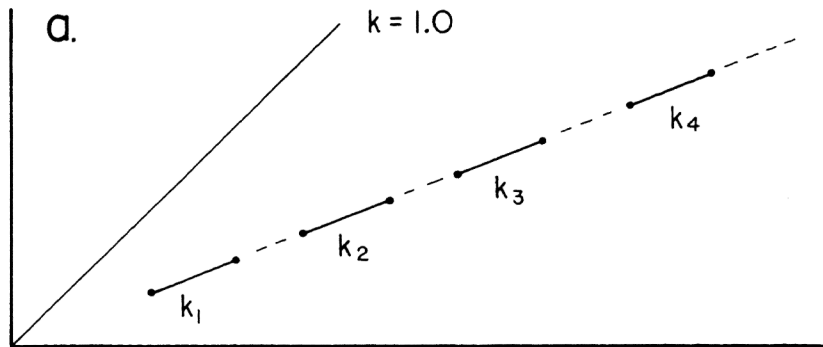


Figure 24. Hypothetical relationships between ontogenetic and interspecific allometry. See text for explanation.





## References

- Alberch, P., S.J. Gould, G.F. Oster and D.B. Wake. 1979.  
Size and shape in ontogeny and phylogeny. *Paleobiology*  
5:296-317.
- Anderson, T.W. 1963. Asymptotic theory for principal  
component analysis. *Ann. Math. Stat.* 34:122-148.
- Bartholemew, G.A. and T.M. Casey. 1978. Oxygen  
consumption of moths during rest, pre-flight warm-up  
and flight in relation to body size and wing  
morphology. *Jour. Exp. Biol.* 76:11-25.
- Bennet, L. 1966. Insect aerodynamics: vertical and  
sustaining force in near-hovering flight. *Science* 152:  
1263- 1266.
- Bennet, L. 1970. Insect flight: lift and rate of  
change of incidence. *Science* 167:177-179.
- Bohart, R.M. and A.S. Menke. 1976. Sphecid wasps of the  
world. University of California Press, Berkeley, Los

Angeles, London.

- Bookstein, F., B. Chernoff, R. Elder, J. Humphries, G. Smith and R. Strauss. 1985. Morphometrics in Evolutionary Biology. Special Publication 15, The Academy of Natural Sciences of Philadelphia.
- Buckholtz, R.H. 1978. Some aspects of unsteady insect aerodynamics: acceleration potential methods in plane unsteady airfoil theory and measurements of unsteady-periodic forces generated by the blowfly. Ph.D. thesis, Johns Hopkins Univ. N79-18903.
- Buckholtz, R.H. 1980. Measurements of unsteady periodic forces generated by the blowfly flying in a wind tunnel. J. Exp. Biol. 90:163-173.
- Calder, W.A. 1984. Size, function and life history. Harvard University Press, Cambridge.
- Casey T.M. and B.A. Joos. 1983. Morphometrics, conductance, thoracic temperature and flight energetics of noctuid and geometrid moths. Physiol. Zool. 56: 160-173.

- Casey, T.M. and M.L. May. 1983. Morphometrics, wing stroke frequency and energy metabolism of euglossine bees during hovering flight. In Biona Report I: Insect Flight (Werner Nachtigall ed.) Gustav Fischer, Stuttgart, NY.
- Casey, T.M., M.L. May and K.R. Morgan. 1985. Flight energetics of euglossine bees in relation to morphology and wing stroke frequency. J. Exp. Biol. 116:271-289.
- Chapman, R.E. 1969. The Insects: Structure and Function. Harvard University Press, Cambridge.
- Clancy, L.J. 1975. Aerodynamics. John Wiley and Sons, New York.
- Cloupeau, M., J.F. Devillers and D. Devezeaux. 1979. Direct measurements of instantaneous lift in desert locust; comparison with Jenson's experiments on detached wings. J. Exp. Biol. 80:1-15.
- Cock, A.G. 1966. Genetical aspects of metrical growth and form in animals. Quart. Rev. Biol. 41:131-191.
- Dalton, S. 1975. Borne on the Wind. Readers

Digest Press, New York.

Dalton, S. 1977. The miracle of flight. Simpson Low,  
London.

Ellington, C.P. 1975. Non-steady-state aerodynamics and  
the flight of Encarsia formosa. In Swimming and Flying  
in Nature (T.Y. Wu, C.J. Brokaw and C. Brennen, eds.)  
vol. 2, pp. 783-796. Plenum Press, New York.

Ellington, C.P. 1984a. The aerodynamics of hovering  
insect flight. Phil. Trans. R. Soc. London (B) 305:1-  
181.

Ellington, C.P. 1984b. The aerodynamics of flapping  
animal flight. Amer. Zool. 24:95-105.

Freedman, L. 1962. Growth of muzzle length relative to  
calvaria length in Papio. Growth 26:117-128.

Fullerton, J.D. 1911. First report of the bird  
construction committee. Aeronautical Society of Great  
Britain.

Galilei, G. 1637. Dialogues Concerning two new sciences

- (translated by H. Crew and A. De Salvio). Macmillan, New York, 1914.
- Gould, S.J. 1966. Allometry and size in ontogeny and phylogeny. *Biol. Rev.* 41:587-640.
- Gould, S.J. 1977. *Ontogeny and phylogeny.* Harvard University Press, Cambridge.
- Greenewalt, C.H. 1960. The wings of insects and birds as mechanical oscillators. *Proc. Am. Phil. Soc.* 104: 605-611.
- Greenewalt, C.H. 1962. Dimensional relationships for flying animals. *Smith. Misc. Coll.* 144:1-46.
- Greenewalt, C.H. 1975. The flight of birds. *Trans. Am. Phil. Soc.* 65:1-67.
- Hertel, H. 1966. *Structure, form, movement.* Reinhold Publ. Co., New York.
- Huxley, J.S. 1932. *Problems of relative growth.* MacVeagh, London.

- Jennrich, R.I. and F.B. Turner. 1969. Measurement of non-circular home range. *J. Theoret. Biol.* 22:227-237.
- Jenson, M. 1956. Biology and physics of locust flight III. The aerodynamics of locust flight. *Phil. Trans. Roy. Soc. London (B)* 239:511-552.
- Jolicoeur, P. 1963a. The degree of robustness of Martes americana. *Growth* 27:1-27.
- Jolicoeur, P. 1963b. The multivariate generalization of the allometric equation. *Biometrics* 19:497-499.
- Jolicoeur, P. and J.E. Mosimann. 1960. Size and shape variation in the painted turtle. A principal component analysis. *Growth* 24:339-354
- Kingsolver, J.G. and M.A.R. Koehl. 1985. Aerodynamics, thermoregulation, and the evolution of insect wings: differential scaling and evolutionary change. *Evolution* 39:488-504.
- Kokshaysky, N.V. 1974. Functional aspects of some details of bird wing configuration. *Syst. Zool.* 22:442-450.

- Kluge, A.G. and R.E. Strauss. 1985. Ontogeny and systematics. *Ann. Rev. Ecol. Syst.* 16:247-268.
- Lande, R. 1979. Quantitative genetic analysis of multivariate evolution applied to brain:body size allometry. *Evolution* 33:402-416.
- Lighthill, M.J. 1973. On the Weis-Fogh mechanism of lift generation. *J. Fluid Mechanics* 60:1-17.
- Lissaman, P.B.S. 1983. Low-Reynolds-number airfoils. *Ann. Rev. Fluid Mech.* 15:223-240.
- MacGillivray, A.D. 1906. A study of the wings of the Tenthredinoidea, a super-family of Hymenoptera. *Proc. U.S. Natl. Museum* 29:569-654.
- Mason, W.R.M. 1986. Standard drawing conventions and definitions for venational and other features of wings of Hymenoptera. *Proc. Ent. Soc. Wash.* 88:1-7.
- Maxworthy, T. 1979. Experiments on the Weis-Fogh mechanism of lift generation by insects in hovering flight Part I. Dynamics of the fling. *J. Fluid Mech.* 93:47-63.

- Maxworthy, T. 1981. The fluid dynamics of insect flight. *Ann. Rev. Fluid Mech.* 13:329-350.
- Nachtigall, W. 1977. Die aerodynamische Polare des Tipula-Flugels und eine Einrichtung zur halbanatomischen Polarenaufnahme. In *Physiology of Movement -- Biomechanics* (Nachtigall, W. ed.), *Fort. Zool.* 24(2-3):13-56.
- Nachtigall, W. 1979. Rasche Richtungsänderung und Torsionen schwingender Fliegenflügel und Hypothesen über zugeordnete instationäre Strömungseffekte. *J. Comp. Physiol.* 133:351-355
- Norberg, R.A. 1972. The pterostigma of insect wings: an inertial regulator of wing pitch. *J. Comp. Physiol.* 81:9-22.
- Peters, R.H. 1983. *Ecological Implications of Body Size.* Cambridge University Press, Cambridge.
- Pringle, J.W.S. 1957. *Insect Flight.* Cambridge University Press, Cambridge.



- Rasnitsyn, A.P. 1979. Origin and Evolution of Lower Hymenoptera. Nauka Publ., Moscow, 1969 (translated from Russian for the Agricultural Research Service, USDA and NSF by Amerind Publ. Co., Put. Ltd., New Delhi).
- Read, D.W. and Lestrel, P.E. 1986. Comment on the uses of homologous-point measures in systematics: a reply to Bookstein et al. Syst. Zool. 35:241-253.
- Rodendorf, B.B. 1949. Evolyutaiya i klassifikatsiya letatal' nogo appatat nasekomykh (Evolution and classification of the wings of insects). Trudy Paleontol. In-ta AN SSSR 16.
- Ross, H.H., 1937. A generic classification of the nearctic sawflies (Hymenoptera, Symphyta). Illinois Biol. Mono. 15:1-173.
- Schmidt-Nielson, K. 1984. Scaling: Why is Animal Size so Important? Cambridge Univ. Press, Cambridge.
- Shea, B.T. 1985. Bivariate and multivariate growth allometry: statistical and biological considerations. J. Zool 206:367-391.

- Simpson, G.G. 1953. The major features of evolution.  
Columbia Univ. Press, New York.
- Somps, C. and M. Luttges 1985. Dragonfly flight: novel  
uses of unsteady separated flows. Science 228:1326-  
1329.
- Sotavolta, O. 1947. The flight-tone (wing-stroke  
frequency) of insects. Acta Ent. Fenn. 4:1-117.
- Sotavolta, O. 1952. The essential factor regulating the  
wing stroke frequency of insects in wing mutilation and  
loading experiments and in experiments at  
subatmospheric pressure. Ann. Zool. Soc. 'Vanamo'  
15:1-67.
- Strauss, R.E. and F.C. Bookstein. 1982. The truss body  
form reconstructions in morphometrics. Syst. Zool.  
31:113-135.
- Vaughan, T.A. 1970. Flight patterns and aerodynamics. In  
(Wimsatt, W.A., ed.), Biology of Bats, vol. 1. Academic  
Press, Dallas.
- Vogel, S.A. 1966. Flight in Drosophila I. Flight

- performance of tethered flies. J. Exp. Biol. 44:567-578.
- Vogel, S.A. 1967a. Flight in Drosophila II. Variations in stroke parameters and wing contour. J. Exp. Biol. 46:383-392.
- Vogel, S.A. 1967b. Flight in Drosophila III. Aerodynamic characteristics of fly wings and wing models. J. Exp. Biol. 46:431-443.
- Vogel, S.A. 1981. Life in Moving Fluids. Princeton University Press, Princeton, N.J.
- Walker, G.T. 1925. The flapping flight of birds I. J. Roy. Aero. Soc. 29:590-594.
- Walker, G.T. 1927. The flapping flight of birds II. J. Roy. Aero. Soc. 31:337-342.
- Warham, J. 1977. Wing loadings, wing shapes and flight capabilities of Procellariiformes. New Zealand J. Zool. 4:73-83.
- Weis-Fogh, T. 1973. Quick estimates of flight fitness

in hovering animals including novel mechanisms for lift production. J. Exp. Biol. 59:169-230.

Wooton, R.J. 1979. Function, homology, terminology in insect wings. Syst. Ent. 4:81-93

Wooton, R.J. 1981. Support and deformability in insect wings. J. Zool., London 193:447-468.